Robotics: Advanced Concepts & Analysis

Module 9 – Modeling and Analysis of Wheeled Mobile Robots

Ashitava Ghosal[1]

[1]Department of Mechanical Engineering
&
Centre for Product Design and Manufacture
Indian Institute of Science
Bangalore 560 012, India
Email: asitava@mecheng.iisc.ernet.in

NPTEL, 2010

1. Contents

2. Lecture 1
   - Wheeled Mobile Robots (WMR) on Flat Terrain

3. Lecture 2*
   - Wheeled Mobile Robots (WMR) on Uneven Terrain

4. Lecture 3*
   - Kinematics and Dynamics of WMR on Uneven Terrain

5. Additional Material
   - Problems, References and Suggested Reading

Outline

1. Contents

2. Lecture 1
   - Wheeled Mobile Robots (WMR) on Flat Terrain

3. Lecture 2*
   - Wheeled Mobile Robots (WMR) on Uneven Terrain

4. Lecture 3*
   - Kinematics and Dynamics of WMR on Uneven Terrain

5. Additional Material
   - Problems, References and Suggested Reading

Contents of Lecture

- Introduction to wheeled mobile robots.
- Different kinds of wheels and their modeling.
- Kinematics of wheeled mobile robots on flat surfaces.
- Modeling of wheel slip.
- Modeling of a WMR with omni-directional wheels.
- Simulation of a WMR with omni-wheels.
- Summary

Introduction

- Previous 8 modules, all robots considered were *stationary* with a *fixed* link or a *base*.
- Several robots are now designed to have *mobility* – They can move on a surface, in water or in air.
- Only robots with capability of mobility on a surface considered.
- Earliest examples are *automated guided vehicles* (AGVs) with wheels used on *flat* factory floors.
- More recently autonomous robots with *legs* and/or a combination or wheels and legs (*hybrid*) have been built.
- Vast majority are *wheeled mobile robots* or WMRs as they are *more efficient* and *faster* than legged or tracked vehicles.
- Legged and tracked vehicles can navigate *rough terrain* more easily.

Introduction

- Autonomous vehicles are used in
  - Industrial environments to move material (parts and finished goods) from one place to another.
  - Military and security applications.
  - Hazardous environments such as inside nuclear reactors or in deep sea bed.
  - Providing mobility to handicapped persons.
  - Planetary exploration.
- Analysis of WMRs involve kinematics, dynamics, control, sensing, motion planning, obstacle avoidance ...
- This lecture *deals* with kinematics and dynamics of WMRs moving on a *flat* surface or a plane.
- Next lecture deals with WMRs moving on uneven or rough terrains.

EXAMPLES OF WMRS

MARS Rover from NASA

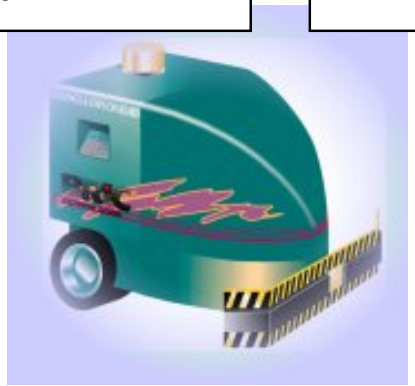


A WMR for moving on uneven terrain



AGV's used on factory floors





A WMR with omni-directional wheels

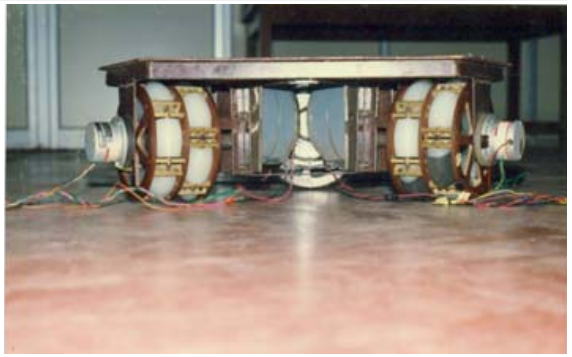


Figure 1: Some Wheeled Mobile Robots

Introduction

- Muir and Newman (1987)
  - A WMR is "a robot capable of locomotion on a surface solely through the wheel assemblies mounted on it and in contact with a surface.
  - A wheel assembly is a device which provides or allow relative motion between its mount and the surface on which it is intended to have single-point of rolling contact".
- In practical wheels, due to deformation, there is *area contact*.
- Different types of wheels used in WMRs – 1) Conventional, 2) Omni-directional and 3) Ball wheels

Introduction

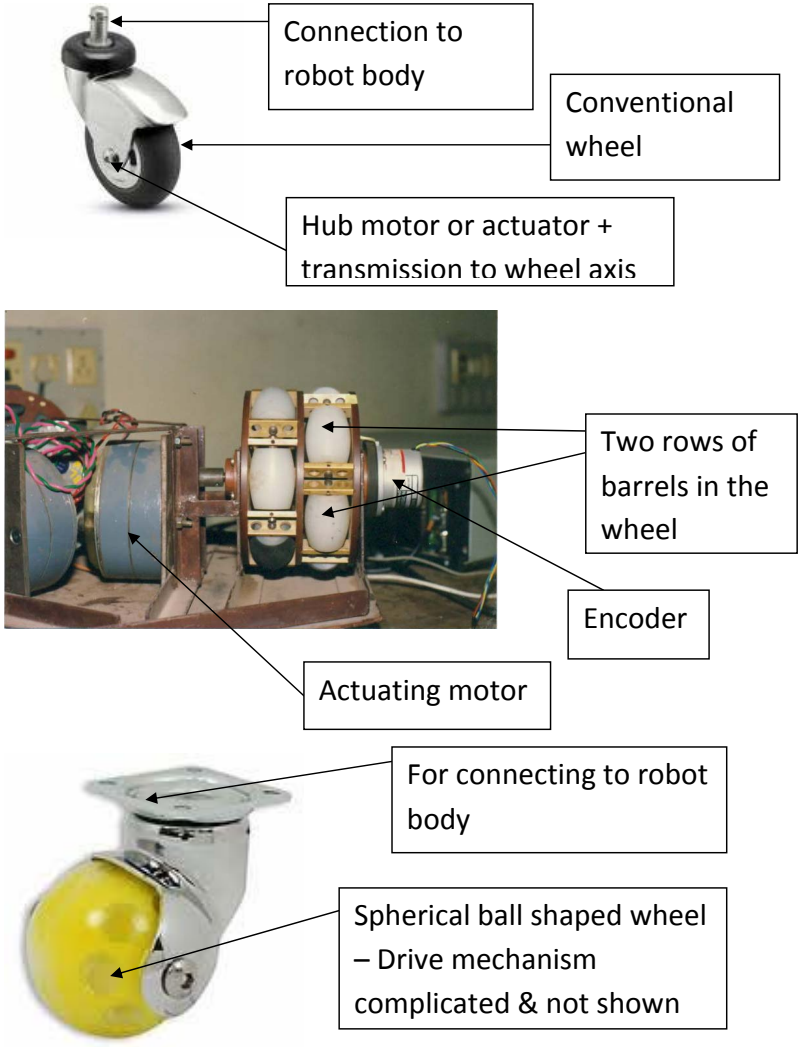
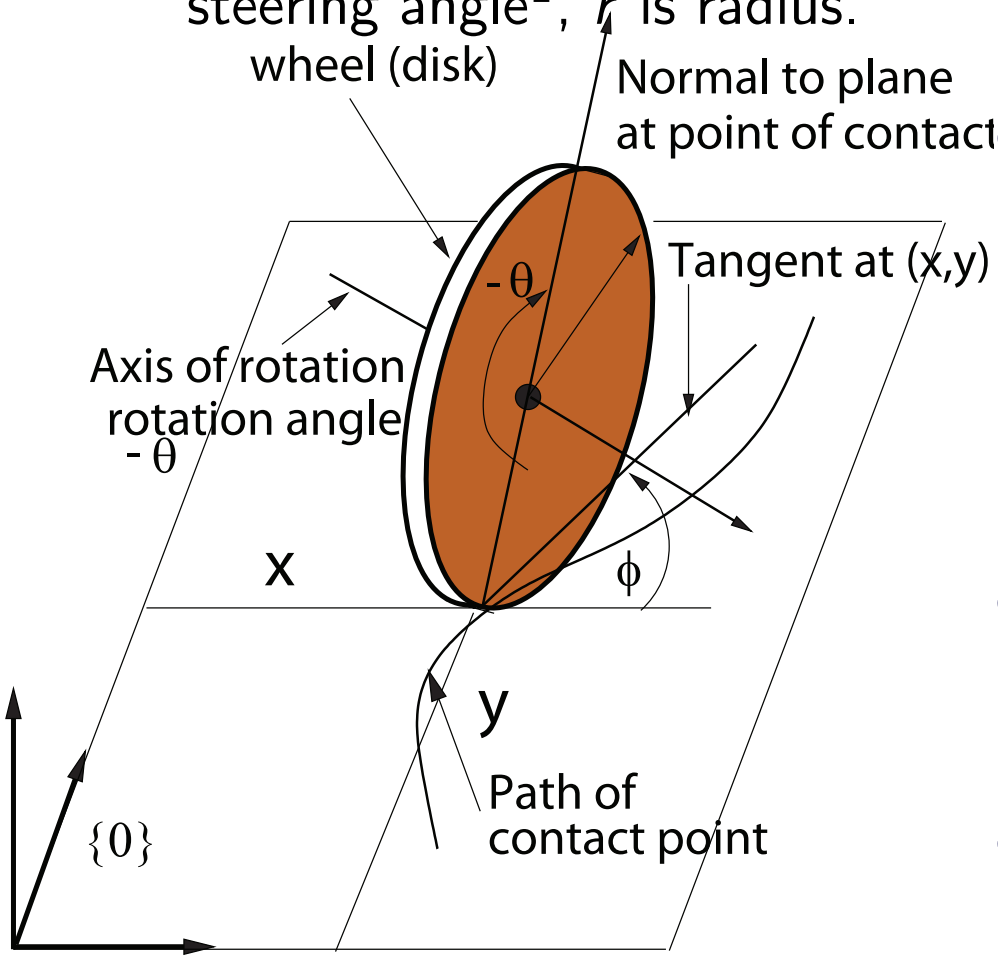


Figure 2: Three main types of wheels in WMR's

- Conventional wheel most commonly used → Rotation about axis of wheel & steering.
- Omni-directional wheels also called Swedish wheels:
  - Barrels on the periphery.
  - Barrel can rotate at an angle to the wheel rotation axis – 90° in figure.
  - Barrel rotation is not actuated & barrel rotation leads to 'sliding' of wheel.
  - Two DOF in each wheel & steering.
- Ball or spherical wheels
  - Essentially a sphere which can rotate about two axis.
  - Complicated drive and rotation measuring arrangement.

Single Wheel Kinematics

- Disk on a plane – Configuration space (x, y, ϕ), ϕ is the steering angle[1], r is radius.



- Wheel rolling without slip – Motion *only* along tangent to path $\dot{x}\sin\phi - \dot{y}\cos\phi = 0$. Velocity perpendicular to the tangent vector is zero.
- *Non-holonomic constraint* – Cannot be integrated to obtain $f(x, y, \phi) = 0$
- Constrains $\dot{\mathbf{q}} = (\dot{x}, \dot{y}, \dot{\phi})^T$, and *not* $\mathbf{q} = (x, y, \phi)^T$.

Figure 3: Wheel rolling on a plane

[1] Tilting of wheel from the normal not considered and rotation of wheel θ not required for analysis. If *thin* disk, tilt must be considered.

Single Wheel Kinematics

- Justification for *non-holonomic nature*
  - Assume $\dot{x}\sin\phi - \dot{y}\cos\phi = 0$ can be integrated.
  - This implies existence of $f(x, y, \phi) = 0 \Rightarrow$ Two DOF $\Rightarrow$ Choosing *any two* out of x, y, ϕ automatically determines the third!
  - For example, at $x = y = 0 \Rightarrow \phi = \phi^*$ is fixed[2] $\Rightarrow$ No other value(s) of ϕ is possible!
  - This is clearly false – Any ϕ is possible at $(0, 0)$ by simply rotating disk about the normal.
  - Hence $f(x, y, \phi) = 0$ is *not integrable*.
- The kinematics of a single wheel is given by

$$\begin{pmatrix} \dot{x} \\ \dot{y} \\ \dot{\phi} \end{pmatrix} = \begin{pmatrix} \cos\phi \\ \sin\phi \\ 0 \end{pmatrix} v + \begin{pmatrix} 0 \\ 0 \\ 1 \end{pmatrix} \omega$$

where v and ω are the forward speed and steering rate.

[2] *At most finitely* many ϕ^* if $f(x, y, \phi) = 0$ is *nonlinear*.

Two Wheel Robot – Bicycle

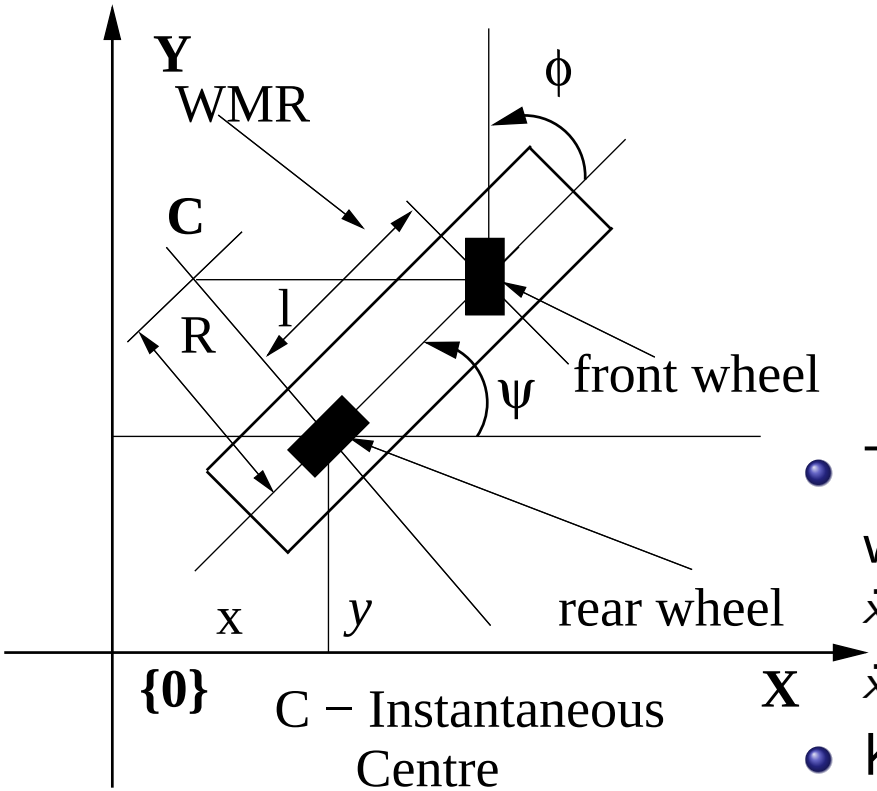


Figure 4: Two wheel robot (bicycle)

- Four generalised coordinates
  - (x, y) – Point of contact of rear wheel.
  - ψ – Orientation of body & rear wheel with X axis.
  - ϕ – Steering angle of front wheel with respect to body
- Two rolling constraints in each wheel:

$$\dot{x}\sin\psi - \dot{y}\cos\psi = 0$$

$$\dot{x}\sin(\psi+\phi) - \dot{y}\cos(\psi+\phi) - l\dot{\psi}\cos\phi = 0$$

- Kinematics equations

$$\begin{pmatrix} \dot{x} \\ \dot{y} \\ \dot{\psi} \\ \dot{\phi} \end{pmatrix} = \begin{pmatrix} \cos\theta\cos\phi \\ \sin\theta\cos\phi \\ \sin\phi/l \\ 0 \end{pmatrix} v_f + \begin{pmatrix} 0 \\ 0 \\ 0 \\ 1 \end{pmatrix} \omega$$

- Lines perpendicular to front and rear wheel velocity vector meet at C.
- Motion of the bicycle is instantaneously rotation about C.

THREE WHEEL ROBOT – TRI-CYCLE

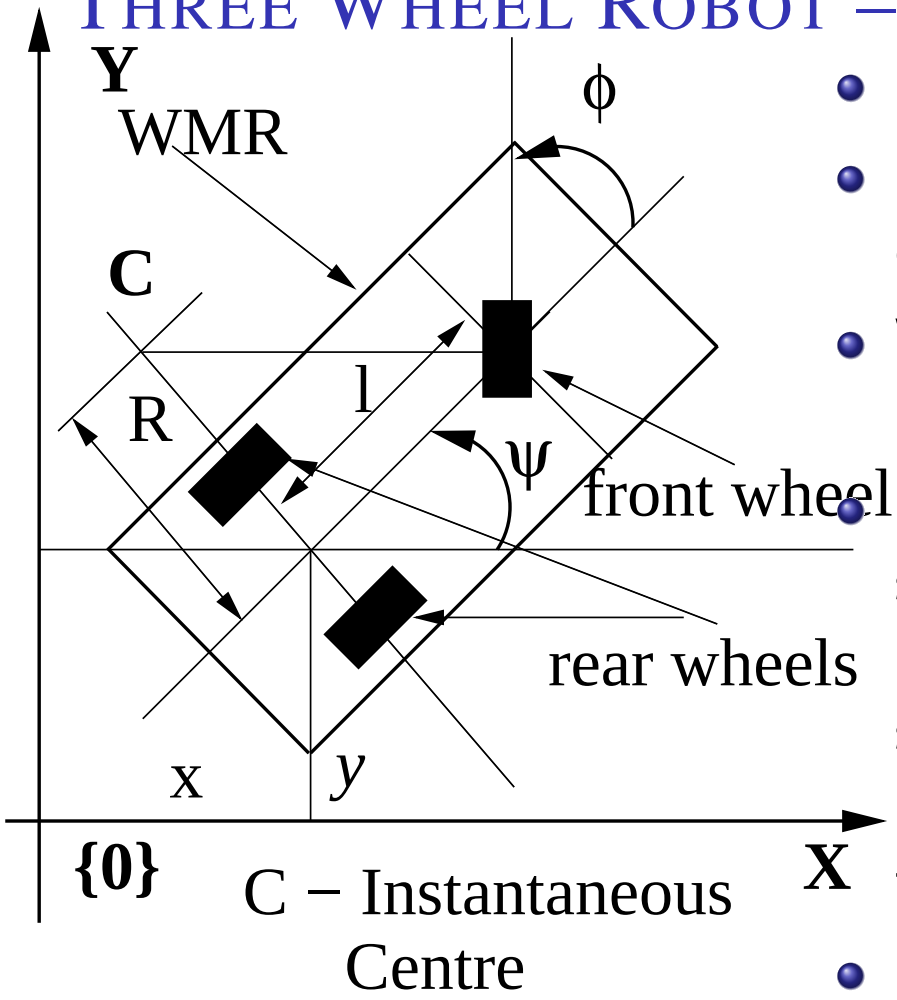


Figure 5: Three wheeled mobile robot or tri-cycle

- Front wheel is steered.
- Speeds of rear wheels are different when making a turn.
- Wheel speed $v_i = \dot{\theta}_i r_i,\ i = 1,2,3,$ r_i is radius of wheel i.
- One rear wheel is driven and the speed of the second rear wheel must adjust so that there is a single instantaneous centre C (the second rear wheel can be free or a differential is used).
- Kinematics of tri-cycle similar to bicycle.

- C determine relation between R, $\dot{\theta}_i$, r_i, l, ψ and ϕ.
- If no single $C \rightarrow$ Wheel(s) slip will occur.

'Car like' Mobile Robots & Others

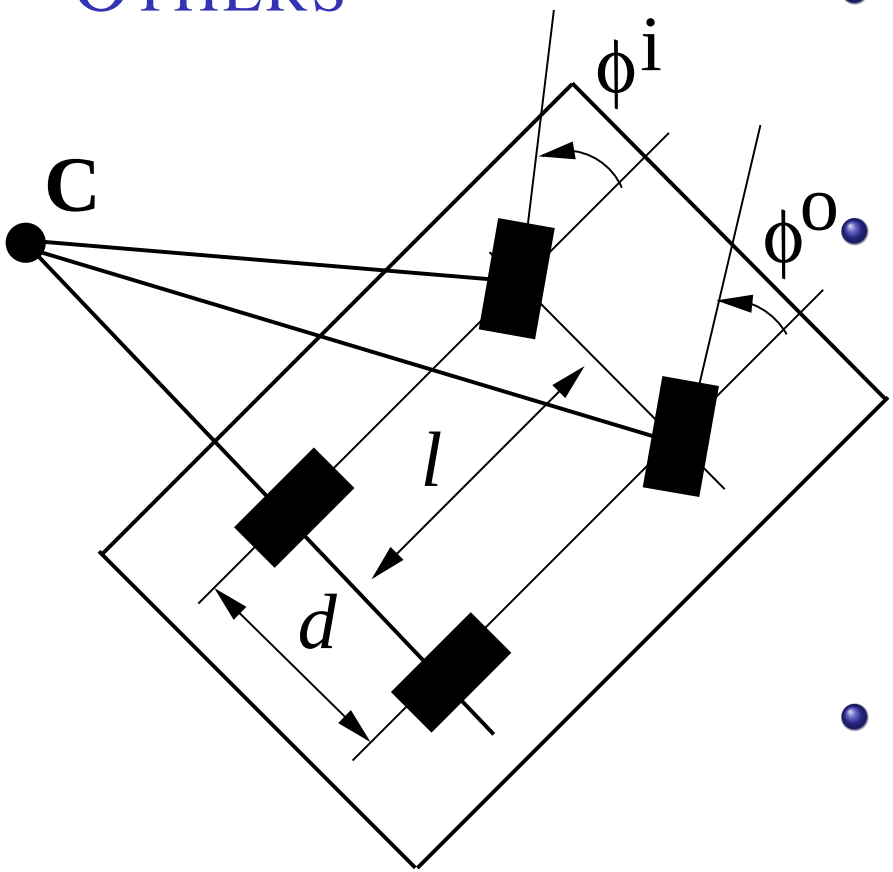


Figure 6: Four-wheeled mobile robot

- Four-wheeled (car like) mobile robot → Steering angle of front wheels is different in a turn.
- Ackerman steering to avoid slippage – The steering angle of 'inside' wheel ϕ^i and 'outside' wheel ϕ^o are related as

$$\cot(\phi^i) - \cot(\phi^o) = d/l$$

- Multi-axle vehicles: truck + trailer
  - Steering front wheel to the 'left' results in 'right' motion of wheels on third axle – *Non-minimum phase* system.
  - More difficult to analyse and model.

Omni-directional wheels

- Six equally spaced 'free' barrels on the periphery.
- Each barrel can rotate about its axis as shown.
- Two rows of barrel $\rightarrow$ One barrel always in contact with ground.
- Distance of point of contact from the vehicle centre changes.

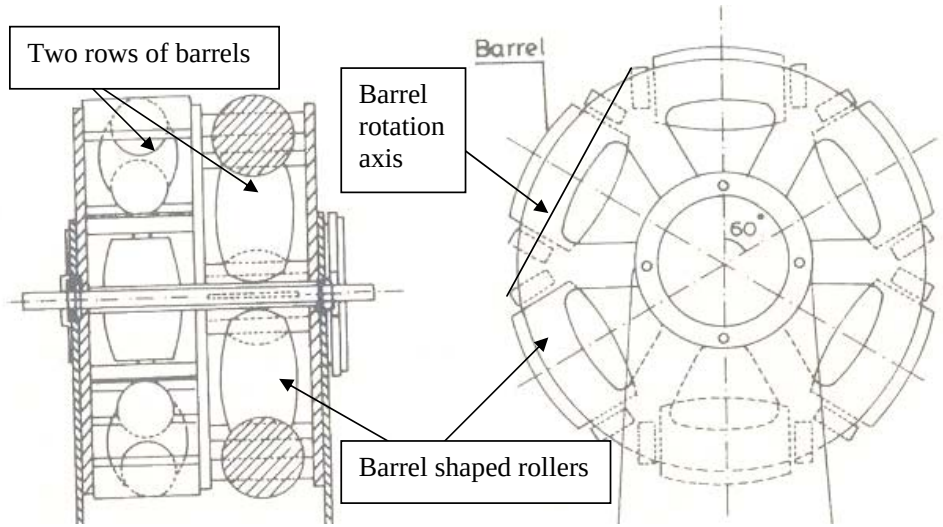


Figure 7: Omni-directional Wheel (Balakrishna & Ghosal, 1995)

- Rotation speed is $\dot{\theta}$ & Sliding speed is σ.
- Two components of velocity of wheel centre for a general case of barrel axis at an angle α to wheel axis – $(r\dot{\theta} + \sigma\cos\alpha, \sigma\sin\alpha)^T$.
- $\alpha = 90^\circ \rightarrow$ Components are $(r\dot{\theta}, \sigma)^T$, r is radius of wheel.

WMR WITH THREE OMNI-WHEELS

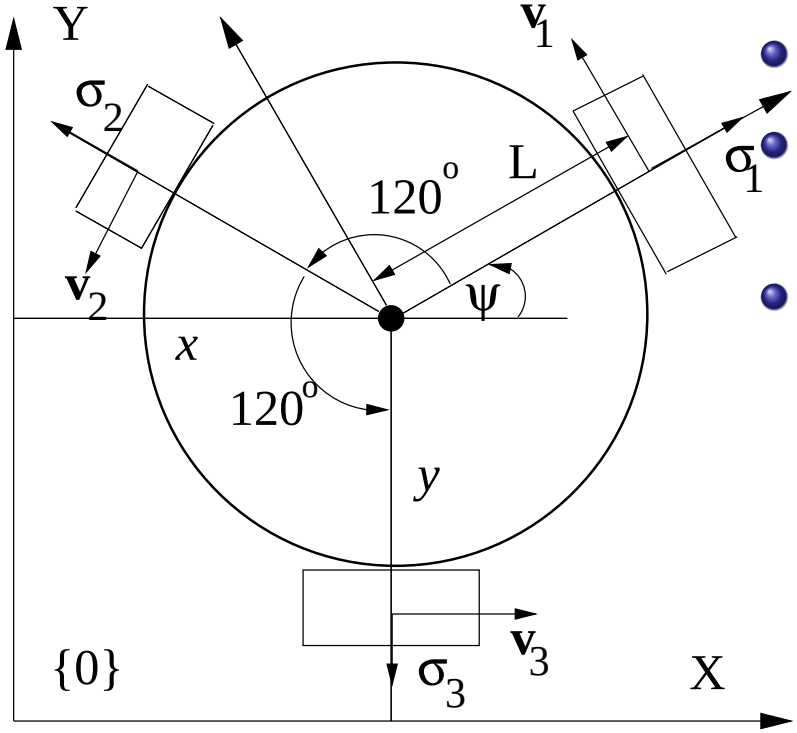


Figure 8: WMR with omni-directional wheels (Balakrishna & Ghosal, 1995)

- WMR with omni-wheels of radius r.
- No steering wheel, wheel rotation speed $\dot{\theta}_i,\ i = 1,2,3$.
- Kinematics – No slip condition at wheels

$$\begin{pmatrix} \dot{\theta}_1 \\ \dot{\theta}_2 \\ \dot{\theta}_3 \end{pmatrix} = \frac{1}{r} \begin{bmatrix} 0 & 1 & L_1 \\ -\sqrt{3}/2 & -1/2 & L_2 \\ \sqrt{3}/2 & -1/2 & L_3 \end{bmatrix} \begin{pmatrix} \dot{x} \\ \dot{y} \\ \dot{\psi} \end{pmatrix}$$

$$= [\ R\ ] \begin{pmatrix} \dot{x} \\ \dot{y} \\ \dot{\psi} \end{pmatrix}$$

$L_i,\ i = 1,2,3$ are the contact points.

- 3×3 matrix $[R]$ (**analogous to manipulator inverse Jacobian**) can be inverted $\rightarrow$ WMR controllable with $\dot{\theta}_i$.
- Can obtain sliding speeds $(\sigma_1, \sigma_2, \sigma_3)^T$ in terms of $(\dot{x}, \dot{y}, \dot{\psi})^T \rightarrow$ Not invertible $\Rightarrow$ WMR cannot be controlled by $\sigma_i,\ i = 1,2,3$ alone.

Modeling of Slip

- For rolling without slip in a conventional wheel of radius r, wheel centre velocity v and wheel angular velocity ω are related by $v = r\omega$.
- Either wheel and/or ground *must deform* for generating *tractive force* to drive a wheel.
- Deformable wheel and/or ground combination $\rightarrow$ Wheel slip will occur (Shekhar, 1997).
- Wheel slip is defined as

$$\lambda = (\dot{\theta} - \omega^*)/y$$

  where $\omega^* \triangleq v/r$ and $\dot{\theta}$ is the wheel angular velocity.
- $y = \omega^*$ when $\omega^* > \dot{\theta}$ and $y = \dot{\theta}$ when $\omega^* < \dot{\theta}*$
- Above implies $-1 \leq \lambda \leq 1$
  - Pure rolling $\rightarrow \lambda = 0$
  - Rolling in place $\rightarrow \lambda = 1$
  - Skidding $\rightarrow \lambda = -1$

Modeling of Slip (Contd.)

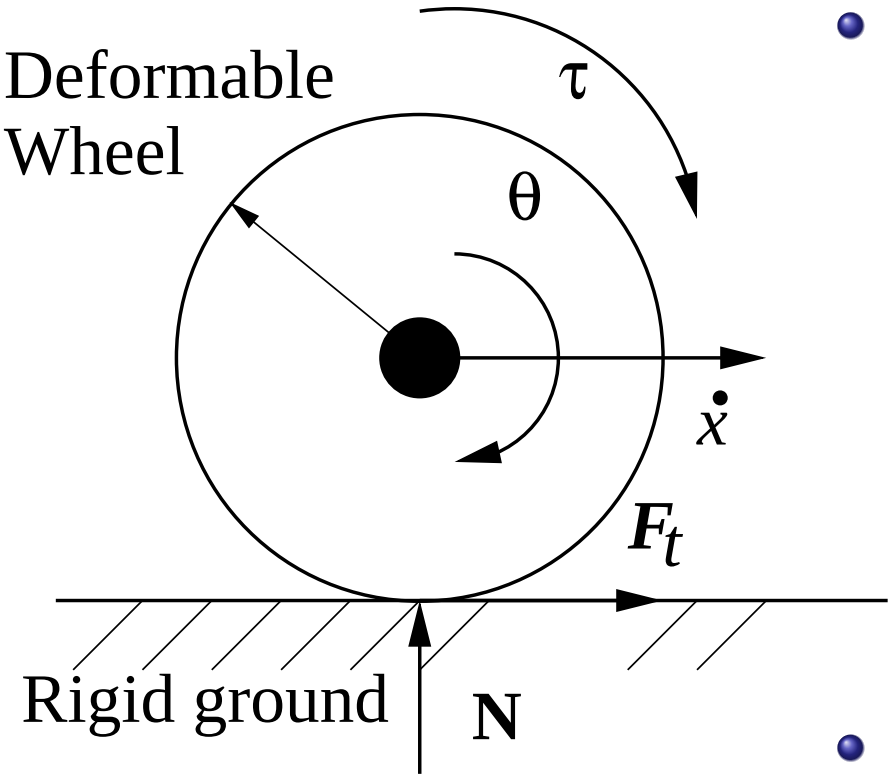


Figure 9: Single wheel dynamics

- Translational and rotation dynamics
  $F_t = M_w \ddot{x}, \quad \tau = J_w \ddot{\theta} + F_t r$
  - F_t: tractive force at wheel-ground interface.
  - τ: torque applied at wheel axle.
  - M_w, J_w: mass and inertia of wheel.
  - $\ddot{x}$, $\ddot{\theta}$: linear and angular acceleration.
- In state-space form
  $\dot{\mathbf{x}} = \mathbf{f}(\mathbf{x}) + \mathbf{g}\tau$
- Lie algebra approach $\rightarrow$ Not *locally* controllable if tractive force F_t is constant.
- F_t *must* be a function of $\dot{x}$ and $\dot{\theta}$.
- F_t is a function of normal reaction **N** and adhesion coefficient μ_a.

Modeling of Slip (Contd.)

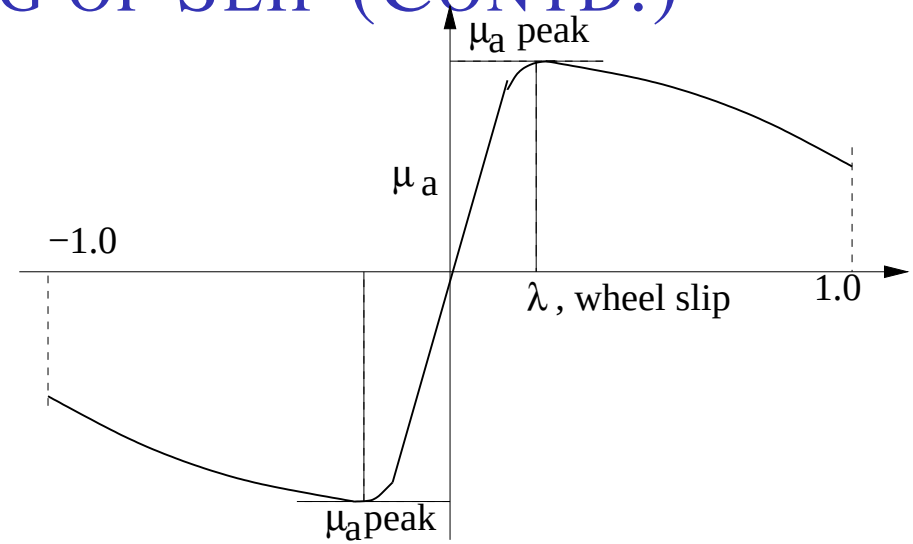


Figure 10: Typical adhesion coefficient Vs wheel slip

- Typically μ_a is a function of wheel slip λ and has a maximum μ_a peak.
- Typical plot shown in figure (Dugoff et al. 1970)
- Tractive force developed $\mathbf{F}_t = \mu_a(\lambda)\mathbf{N}$
- Actually $0 < |\mathbf{F}_t| \leq \mu_a \mathbf{N}$: Proper sign of $\mathbf{F}_t$ for acceleration or braking.
- Stable region – Increasing μ_a with wheel slip.
- After μ_a peak, tractive force falls with increasing wheel slip $\rightarrow$ Unstable!

Equations of Motion

- Equations of motion using Lagrangian formulation (see Balakrishna & Ghosal, 1995)
  - Kinetic energy of platform of mass M_p and inertia I_p.
  - Kinetic energy of wheels of inertia I_i, $i = 1, 2, 3$.
  - No potential energy as motion on flat plane.
- Including tractive forces at wheels F_{t_i}, torque at each wheel τ_i and an approximate μ_a Vs λ curve.
- Equations of motion – 6 ODE's to take into account slip

$$\begin{bmatrix} M_p & 0 & 0 \\ 0 & M_p & 0 \\ 0 & 0 & I_p \end{bmatrix} \begin{pmatrix} \ddot{x} \\ \ddot{y} \\ \ddot{\psi} \end{pmatrix} + \dot{\psi} \begin{bmatrix} 0 & -M_p & 0 \\ M_p & 0 & 0 \\ 0 & 0 & 0 \end{bmatrix} \begin{pmatrix} \dot{x} \\ \dot{y} \\ \dot{\psi} \end{pmatrix} = r \, [\, R \,]^T \begin{pmatrix} F_{t_1} \\ F_{t_2} \\ F_{t_3} \end{pmatrix}$$

$$\begin{bmatrix} I_1 & 0 & 0 \\ 0 & I_2 & 0 \\ 0 & 0 & I_3 \end{bmatrix} \begin{pmatrix} \ddot{\theta}_1 \\ \ddot{\theta}_2 \\ \ddot{\theta}_3 \end{pmatrix} + r \begin{pmatrix} F_{t_1} \\ F_{t_2} \\ F_{t_3} \end{pmatrix} = \begin{pmatrix} \tau_1 \\ \tau_2 \\ \tau_3 \end{pmatrix}$$

CONTROL

- Desired Cartesian path $\mathbf{X}_d = (x_d(t), y_d(t), \psi_d(t))^T$ prescribed.
- PID control

$$\mathscr{F} = [K_v]\,(\dot{\mathbf{X}}_d - \dot{\mathbf{X}}) + [K_p]\,(\mathbf{X}_d - \mathbf{X}) + [K_i] \int (\mathbf{X}_d - \mathbf{X})\, d\tau$$

  $\mathbf{X} = (x(t),\, y(t),\, \psi(t))^T$.
- Cartesian forces $\mathscr{F}$ is related to (wheel) actuator torque by

$$\tau = [\ R\ ]^{T^{-1}}\ \mathscr{F}$$

- Model based control scheme (see Module 7, Lecture 3) using 'ideal' rolling – $\tau = [\alpha]\,\tau' + \beta$ where

$$\begin{aligned} [\alpha] &= [\ R\ ]^{-T}\,[M^*], \quad \beta = [\ R\ ]^{-T}\,\{\dot{\psi}\,[\ Q\ ]\,\dot{\mathbf{X}}\} \\ \tau' &= \ddot{\mathbf{X}}_d + K_v(\dot{\mathbf{X}}_d - \dot{\mathbf{X}}) + K_p(\mathbf{X}_d - \mathbf{X}) \end{aligned}$$

  where $[M^*] = ([M] + [\ R\ ]^T\,[I]\,[\ R\ ])$ is the mass matrix corresponding to 'ideal' rolling.

NUMERICAL SIMULATION RESULTS

- Geometry of WMR: $L_1 = L_2 = L_3 = 0.5$ m, $r = 0.1$ m
- Inertia parameters: $M_p = 50.0$ Kg, $I_p = 5.0$ kg m^2, $I_i = 2.0$ kg m^2.
- Controller gains equal: $K_{p_i} = 15.0$, $K_{v_i} = 2\sqrt{K_{p_i}}$, and $K_{i_i} = 0.10$.

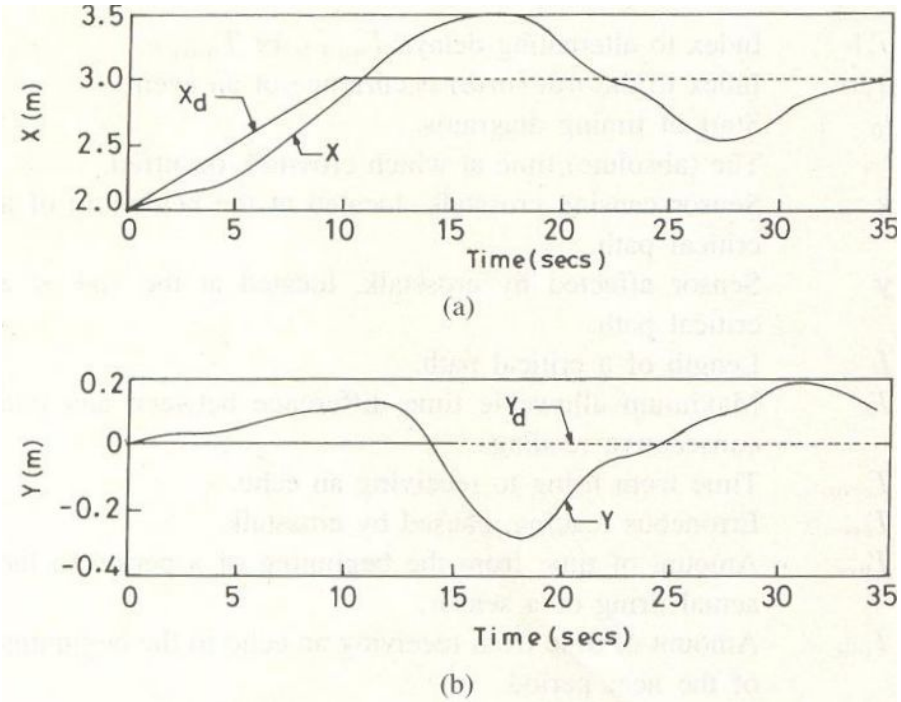


Figure 11: Straight line trajectory control using PID controller (Balakrishna & Ghosal, 1995)

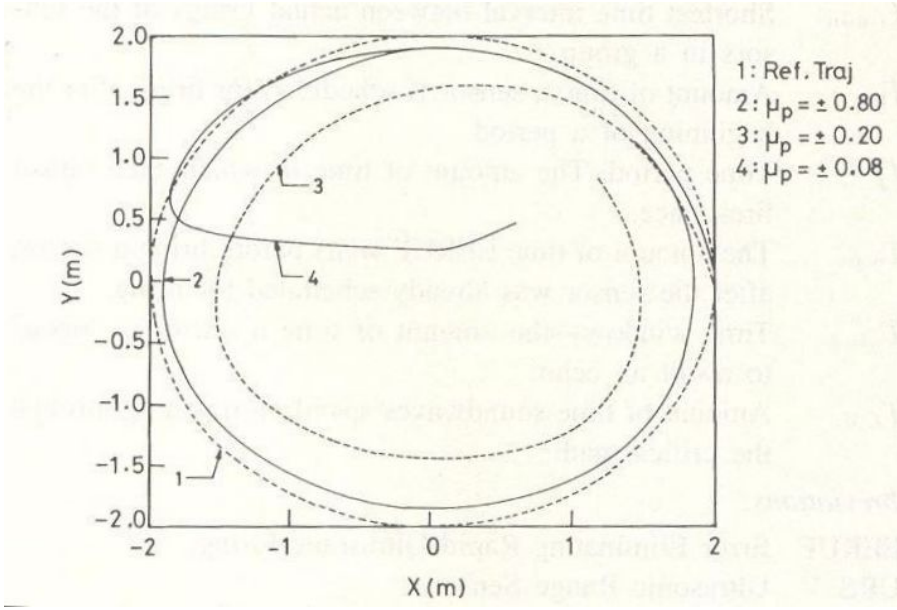


Figure 12: Circular trajectory control using model-based controller (Balakrishna & Ghosal, 1995)

Numerical simulation results (Contd.)

- Performance of PID controller is quite poor.
- Maximum x error is approximately 0.5 m and maximum y error is approx 0.2 m.
- Model based controller using 'ideal' rolling as model performs slightly better.
- As the μ_a peak decreases from 0.8 to 0.08, performance of model based controller becomes poorer.
- Maximum radial error from desired circular trajectory of radius 2.0 m is approximately 1.7 m.
- It is important to model or take into account slip in WMR models. This is also borne out by experiments!

Summary of Modeling of WMR

- WMR modeling and analysis is very different from serial and parallel manipulators.
  - Base is not fixed.
  - Wheel-ground contact results in *non-holonomic* constraints – Compare with *holonomic* in joints.
  - Non-holonomic constraints *does not* restrict the configuration space but *restrict* space of velocities!
- Various kinds of wheels in use – Conventional, omni-directional and ball wheels.
  - Conventional wheels rotate about the wheel axis and can be steered about the normal.
  - Omni-directional wheel can rotate about its axis, slide along another direction and also steered.
  - Ball wheels can rotate about two different axis.
- WMR with three wheels simplest – Four wheeled and multi-axle WMR's more difficult to model and analyse.
- Slip, due to deformation, always present in wheels $\rightarrow$ Need to be taken into account in WMR dynamics and control.

Outline

1. Contents

2. Lecture 1
   - Wheeled Mobile Robots (WMR) on Flat Terrain

3. Lecture 2*
   - Wheeled Mobile Robots (WMR) on Uneven Terrain

4. Lecture 3*
   - Kinematics and Dynamics of WMR on Uneven Terrain

5. Additional Material
   - Problems, References and Suggested Reading

Contents of Lecture

- Introduction
- Modeling of torus-shaped wheel and uneven terrain
- Single wheel on uneven terrain – Kinematic and dynamic modeling and simulation.
- A WMR for traversing uneven terrain without slip.
- Summary

Introduction

- Most WMR are used in industrial environments – Flat & structured surfaces.
- Recent interest in uneven and rough terrains & off-road environments.
  - Planetary exploration.
  - DARPA Grand Challenge to develop a fully autonomous ground vehicle capable of completing a off-road course in limited time (see link[3] for more details).
  - Luxury cars.
- Flat terrain – Vehicle platform has 3 DOF consisting of position (x, y) and orientation ψ
- Uneven terrain – Vehicle platform can possibly have all three components of translation and three components of orientation $\rightarrow$ Up to 6 DOF.

[3] Copy and paste link in a *New Window/Tab* by *right click*. Close *New Window/Tab* after viewing.

INTRODUCTION

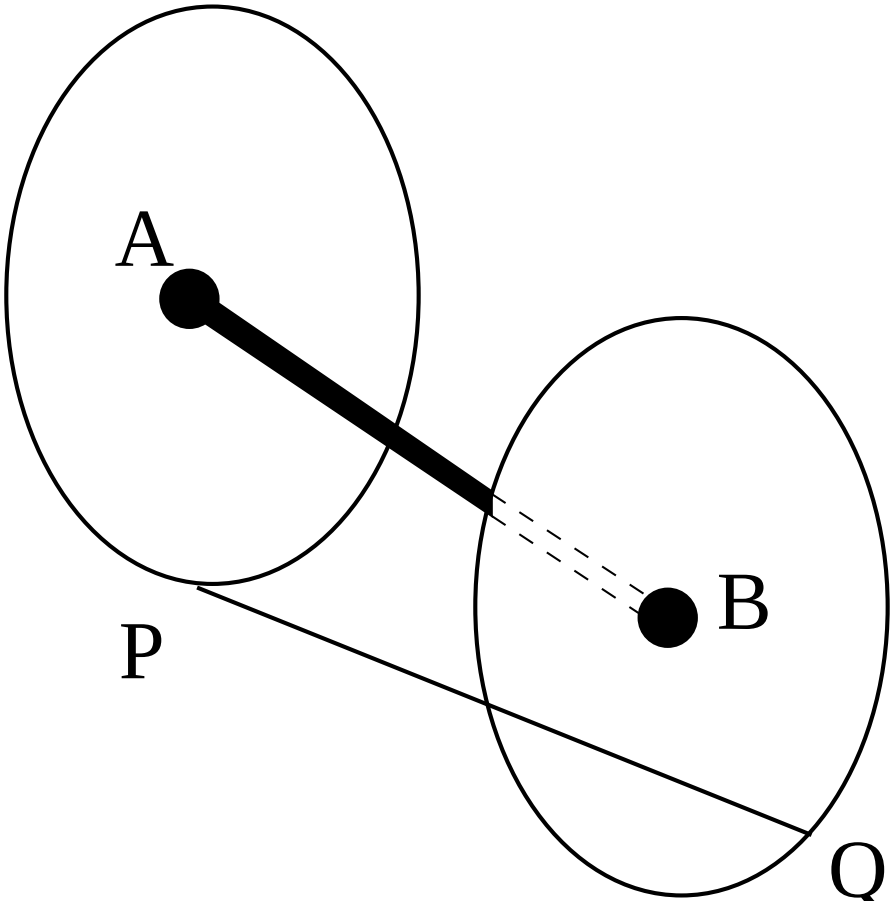


Figure 13: Wheel slip on uneven terrain

- Two wheels connected by a *fixed* length axle AB.
- Points of contact with *uneven ground* P, Q can change $\rightarrow$ Length PQ is variable and *not equal* to AB.
- Variation of length PQ require a velocity component along axle AB and along the normal (Waldron, 1995).
- No instantaneous centre compatible with both wheels $\Rightarrow$ Wheel slip will occur.
- Wheel slip leads to a) localization errors, and b) wastage of fuel.

Introduction

- To overcome wheel slip $\rightarrow$ Variable length axle (Choi & Sreenivasan, 1999).
- Add *passive* prismatic joint in axle – Prismatic joint changes axle length by required amount to ensure compatible instantaneous centre for both wheels.
- At large inclination, gravity causes prismatic joint to change length in undesired way!
- Actuated (and controlled) prismatic joint – Accurate sensing of slip is required.
- New concept of WMR capable of traversing uneven terrain without slip.

Introduction

- Main concepts (see Chakraborty & Ghosal (2004, 2005)).
  - Use of torus shaped wheel – Wheel has single point contact with uneven terrain.
  - Torus shaped wheels connected to WMR body with passive rotary joints.
  - Passive rotary joint allow lateral tilting and wheel-ground contact distance (PQ) to change.
  - Three actuated joints (for a 3DOF model) in WMR.
  - Rear wheels are driven and can tilt laterally.
  - Front wheel steered and can roll *freely*.
- Use of contact equations (Montana, 1988) to model wheel-ground contact.
- WMR modeled as a parallel robot at each instant.

MODELING OF SURFACE

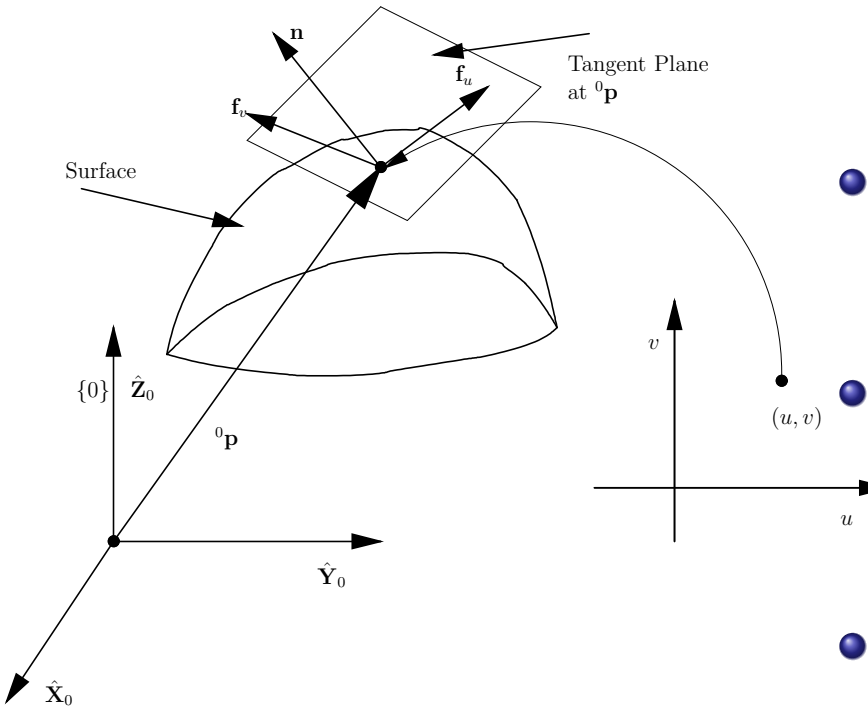


Figure 14: A surface in $\Re^3$

- A surface in $\Re^3$ can be represented in parametric form $(x, y, z)^T = \mathbf{f}(u, v)$, $(u, v) \in U \subseteq \Re^2$ maps to ${}^0\mathbf{p} = (x, y, z)^T$ on the surface.
- At a point, tangent plane defined by vectors $\mathbf{f}_u = \dfrac{\partial \mathbf{f}}{\partial u}$ and $\mathbf{f}_v = \dfrac{\partial \mathbf{f}}{\partial v}$.
- The normal to the surface is $\mathbf{n} = \dfrac{\mathbf{f}_u \times \mathbf{f}_v}{|\mathbf{f}_u \times \mathbf{f}_v|}$
- The vectors $\dfrac{\mathbf{f}_u}{|\mathbf{f}_u|}$, $\dfrac{\mathbf{f}_v}{|\mathbf{f}_v|}$, and $\mathbf{n}$ form a right-handed basis[a] at ${}^0\mathbf{p}$.

[a] If $\mathbf{f}_u$ and $\mathbf{f}_v$ are not orthogonal, then the orthogonal set is $\{\mathbf{f}_u/|\mathbf{f}_u|, \mathbf{n} \times \mathbf{f}_u/|\mathbf{f}_u|, \mathbf{n}\}$.

Modeling of a Torus-shaped Wheel

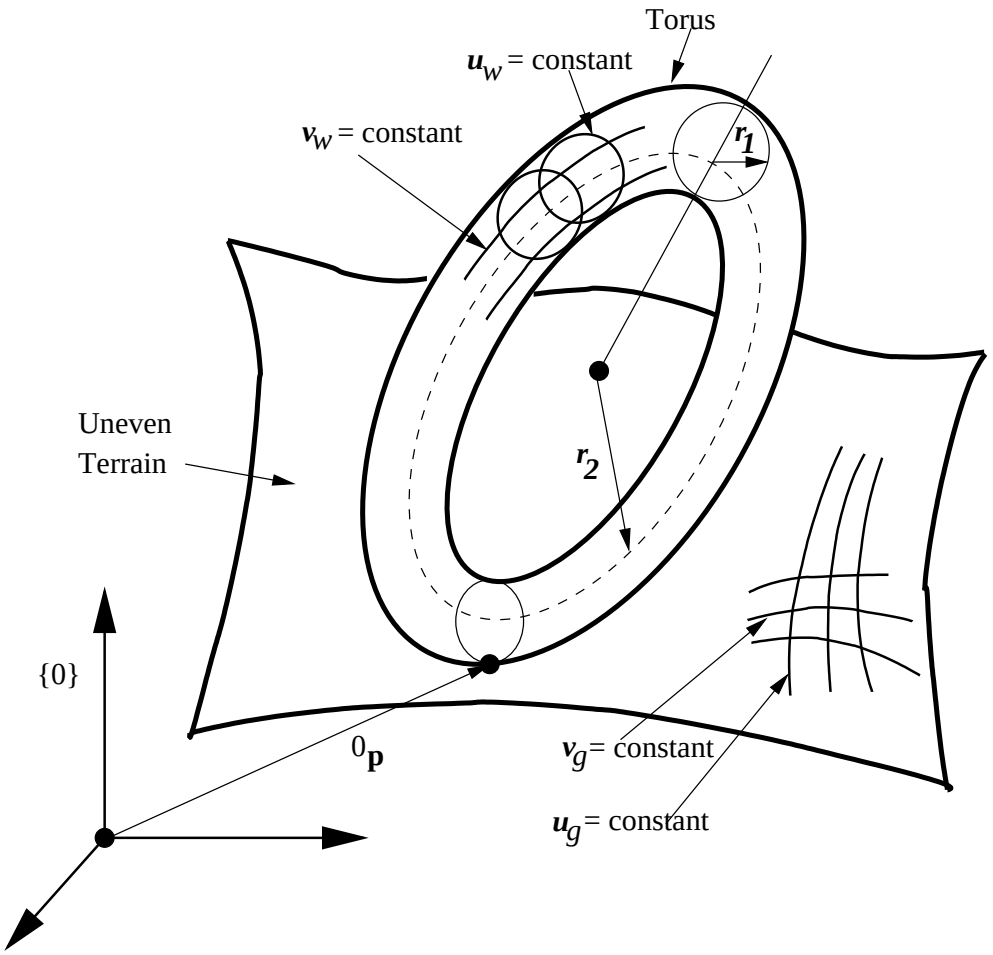


Figure 15: A torus-shaped wheel on uneven terrain

- Equation of a torus in parametric form

$$\begin{aligned} x &= r_1 \cos u_w \\ y &= \cos v_w (r_2 + r_1 \sin u_w) \\ z &= \sin v_w (r_2 + r_1 \sin u_w) \end{aligned}$$

- r_1 and r_2 are the two radii associated with a torus.
- Subscript w on the parameters u and v denote a wheel.
- Uneven terrain/ground $(x, y, z)^T = \mathbf{f}(u_g, v_g)$

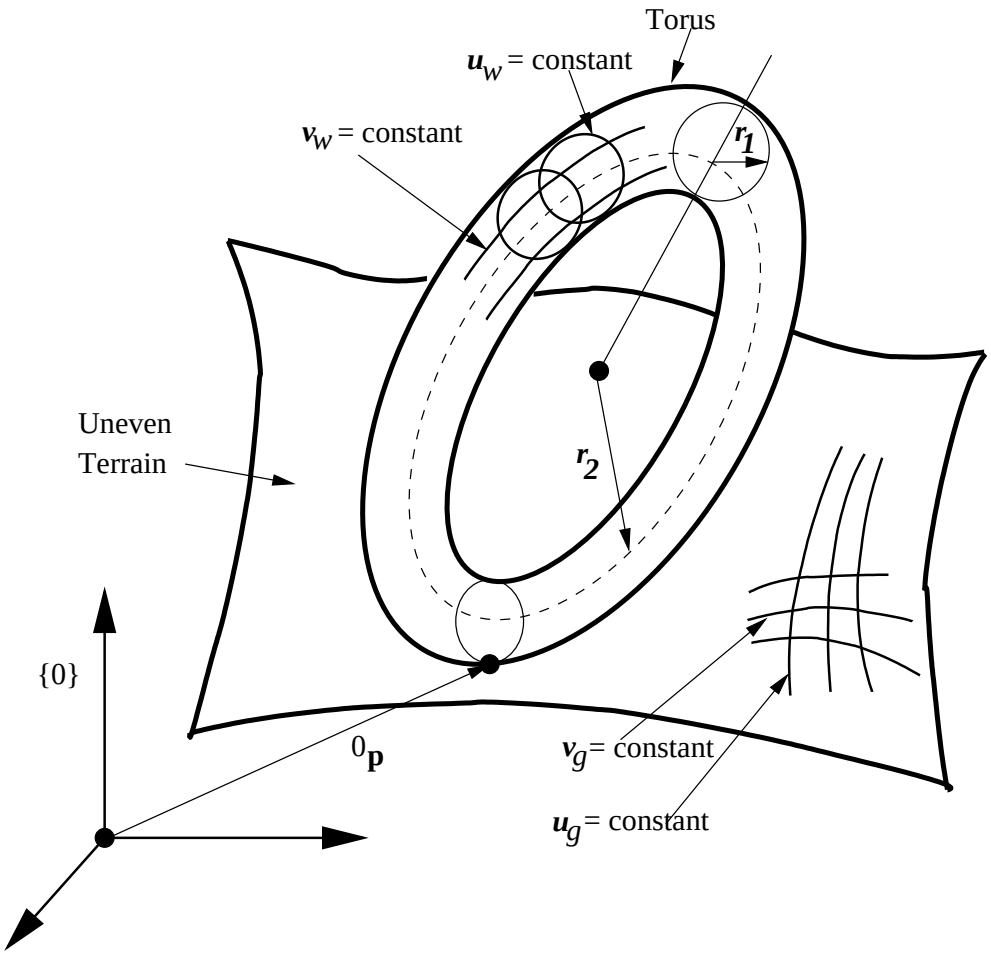
Metric, Curvature and Torsion of a Surface

- From the parametric equation, define
  - Second partial of $\mathbf{f}$, $\mathbf{f}_{(\cdot)(\cdot)} = \dfrac{\partial^2 \mathbf{f}}{\partial(\cdot)\partial(\cdot)}$, with respect to u and v,
  - Partial of $\mathbf{n}$, $\mathbf{n}_{(\cdot)}$, with respect to u and v.
  - Metric on a surface $[\mathbf{M}] = \begin{bmatrix} |\mathbf{f}_u| & 0 \\ 0 & |\mathbf{f}_v| \end{bmatrix}$
  - Curvature form

$$[\mathbf{K}] = \begin{bmatrix} \frac{\mathbf{f}_u \cdot \mathbf{n}_u}{|\mathbf{f}_u|^2} & \frac{\mathbf{f}_u \cdot \mathbf{n}_v}{|\mathbf{f}_u||\mathbf{f}_v|} \\ \\ \frac{\mathbf{f}_v \cdot \mathbf{n}_u}{|\mathbf{f}_u||\mathbf{f}_v|} & \frac{\mathbf{f}_v \cdot \mathbf{n}_v}{|\mathbf{f}_v|^2} \end{bmatrix}$$

  - Torsion form $[\mathbf{T}] = \begin{bmatrix} \dfrac{\mathbf{f}_v \cdot \mathbf{f}_{uu}}{|\mathbf{f}_u|^2|\mathbf{f}_v|} & \dfrac{\mathbf{f}_v \cdot \mathbf{f}_{uv}}{|\mathbf{f}_v|^2|\mathbf{f}_u|} \end{bmatrix}$
- Metric 'defines' distance, Curvature determines 'in-plane' bending and Torsion determines 'out-of-plane' bending on a surface.

Modeling of a Torus-shaped Wheel



- For the torus-shaped wheel

$$[\mathbf{M}_w] = \begin{bmatrix} r_1 & 0 \\ 0 & r_2 + r_1 \sin u_w \end{bmatrix}$$

$$[\mathbf{K}_w] = \begin{bmatrix} \frac{1}{r_1} & 0 \\ 0 & \frac{\sin u_w}{r_2 + r_1 \sin u_w} \end{bmatrix}$$

$$[\mathbf{T}_w] = \begin{bmatrix} 0 & \frac{\cos u}{r_2 + r_1 \sin u_w} \end{bmatrix}$$

Figure 16: A torus-shaped wheel on uneven terrain

Modeling of Uneven Terrain

- Uneven terrain – Smooth and hard, *not* terrains with sand, dirt or any discontinuities!
- Explicit or parametric equation not available.
- Local elevation of a point is known from measurement (laser scanner).
- Ill-posed problem to obtain $\mathbf{f}(u, v)$ from measurements– *Non-uniqueness*.
- Use bi-cubic and B-spline surfaces (see Mortenson, 1985)
  - Bi-cubic surface patch:
    $\mathbf{f}(u, v) = \sum_{i=0}^{3} \sum_{j=0}^{3} a_{ij} u^i v^j, \quad (u, v) \in [0, 1]$
  - Can be determined from 4 corner points of the patch.
  - Patches can be smoothly connected to make up the whole surface.
  - Higher-order continuity can be obtained by using Non-uniform Rational B-Spline (NURBS)
- MATLAB® Spline Toolbox – Partial derivatives of surface available to compute metric, curvature and torsion form.

EXAMPLES OF UNEVEN TERRAINS

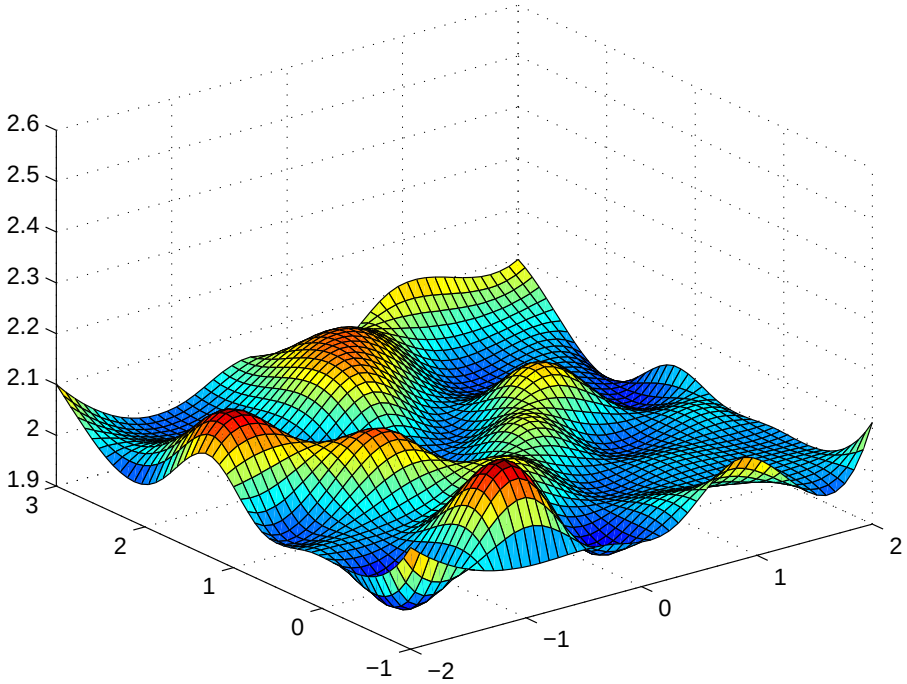


Figure 17: A bi-cubic uneven surface

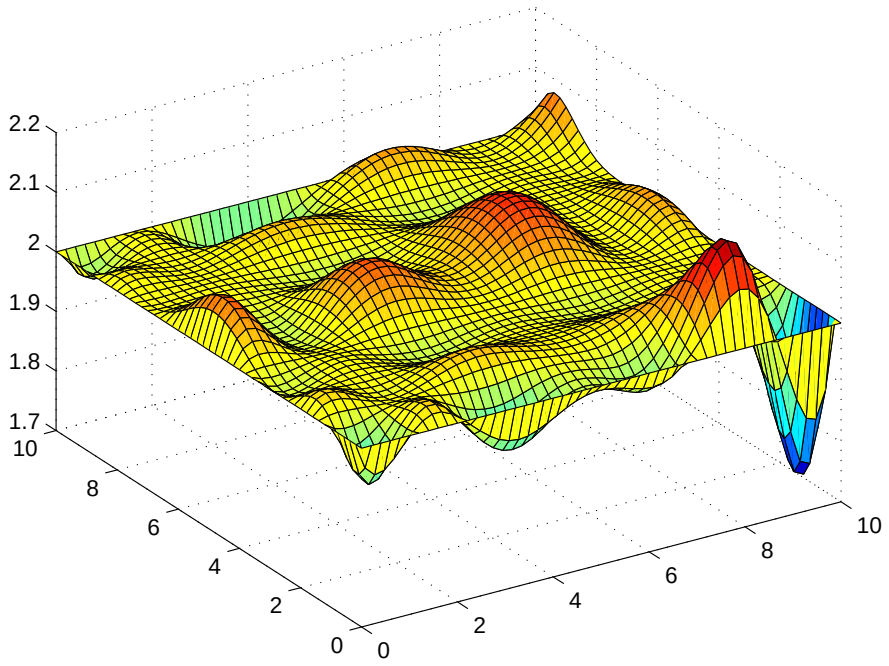


Figure 18: A B-spline uneven surface

KINEMATICS OF CONTACT

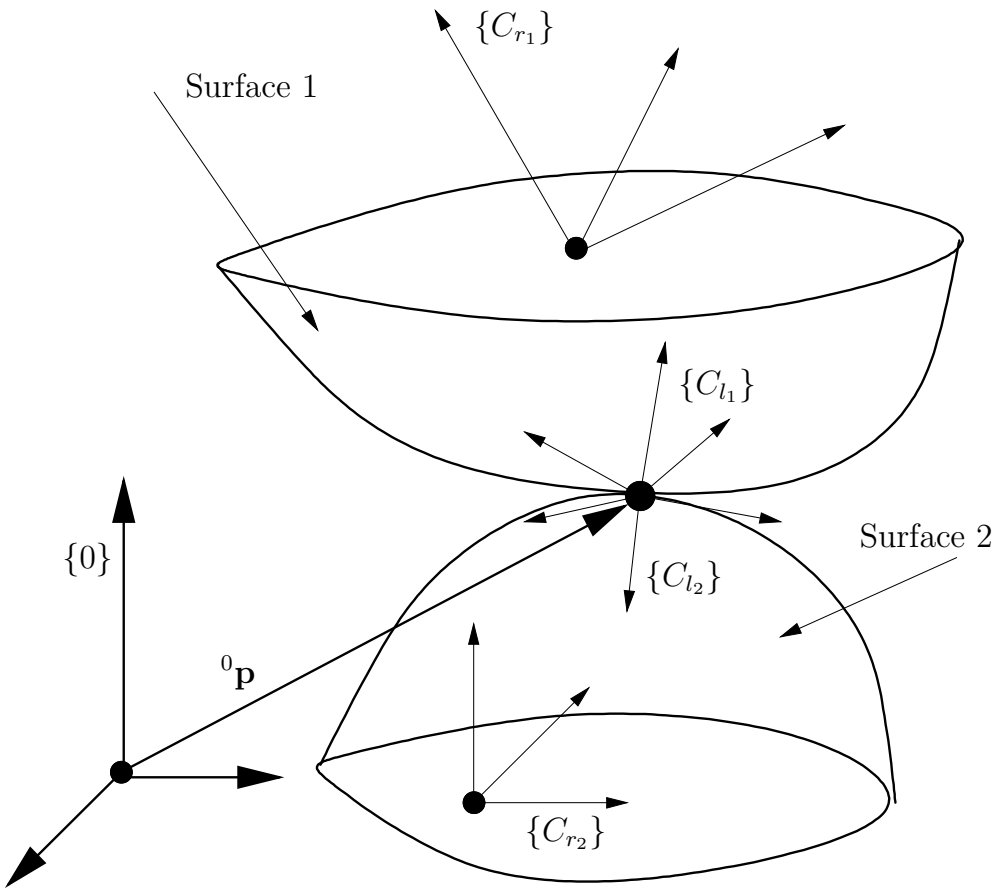


Figure 19: Two arbitrary surfaces in single-point contact

- Two surfaces 1 and 2 described with respect to $\{C_{r_1}\}$ and $\{C_{r_2}\}$.
- Parametric equations are $\mathbf{f}(u_1, v_1)$ and $\mathbf{f}(u_2, v_2)$.
- At point of contact ${}^0\mathbf{p}$, fix frames $\{C_{l_1}\}$ and $\{C_{l_2}\}$.
- ψ – Angle between X axis of $\{C_{l_1}\}$ and $\{C_{l_2}\}$.
- (u_1, v_1), (u_2, v_2) and ψ define the 5 DOF for single-point contact.
- Define metric, $[M]$, Curvature $[K]$ and Torsion $[T]$ for the two surfaces at ${}^0\mathbf{p}$.

KINEMATICS OF CONTACT

- Contact equations: Relationship between $(\dot{u}_1, \dot{v}_1, \dot{u}_2, \dot{v}_2, \dot{\psi})$ and the linear and angular velocity components v_x, v_y, v_z and $\omega_x, \omega_y, \omega_z$

$$
\begin{aligned}
(\dot{u}_1, \dot{v}_1)^T &= [\mathbf{M}_1]^{-1}([\mathbf{K}_1]+[\mathbf{K}^*])^{-1}[(-\omega_y, \omega_x)^T - [\mathbf{K}^*](v_x, v_y)^T] \\
(\dot{u}_2, \dot{v}_2)^T &= [\mathbf{M}_2]^{-1}[R_\psi]([\mathbf{K}_1]+[\mathbf{K}^*])^{-1}[(-\omega_y, \omega_x)^T + [\mathbf{K}_1](v_x, v_y)^T] \\
\dot{\psi} &= \omega_z + [\mathbf{T}_1][\mathbf{M}_1](\dot{u}_1, \dot{v}_1)^T + [\mathbf{T}_2][\mathbf{M}_2](\dot{u}_2, \dot{v}_2)^T \\
0 &= v_z
\end{aligned}
$$

where the *relative* curvature of surface 2 with respect to 1 is $[\mathbf{K}^*] = [R_\psi][\mathbf{K}_2][R_\psi]^T$ and the rotation matrix $[R]$ is

$$
[R_\psi] = \begin{pmatrix} \cos\psi & -\sin\psi \\ -\sin\psi & -\cos\psi \end{pmatrix}
$$

KINEMATICS OF CONTACT

- Can also invert the equations

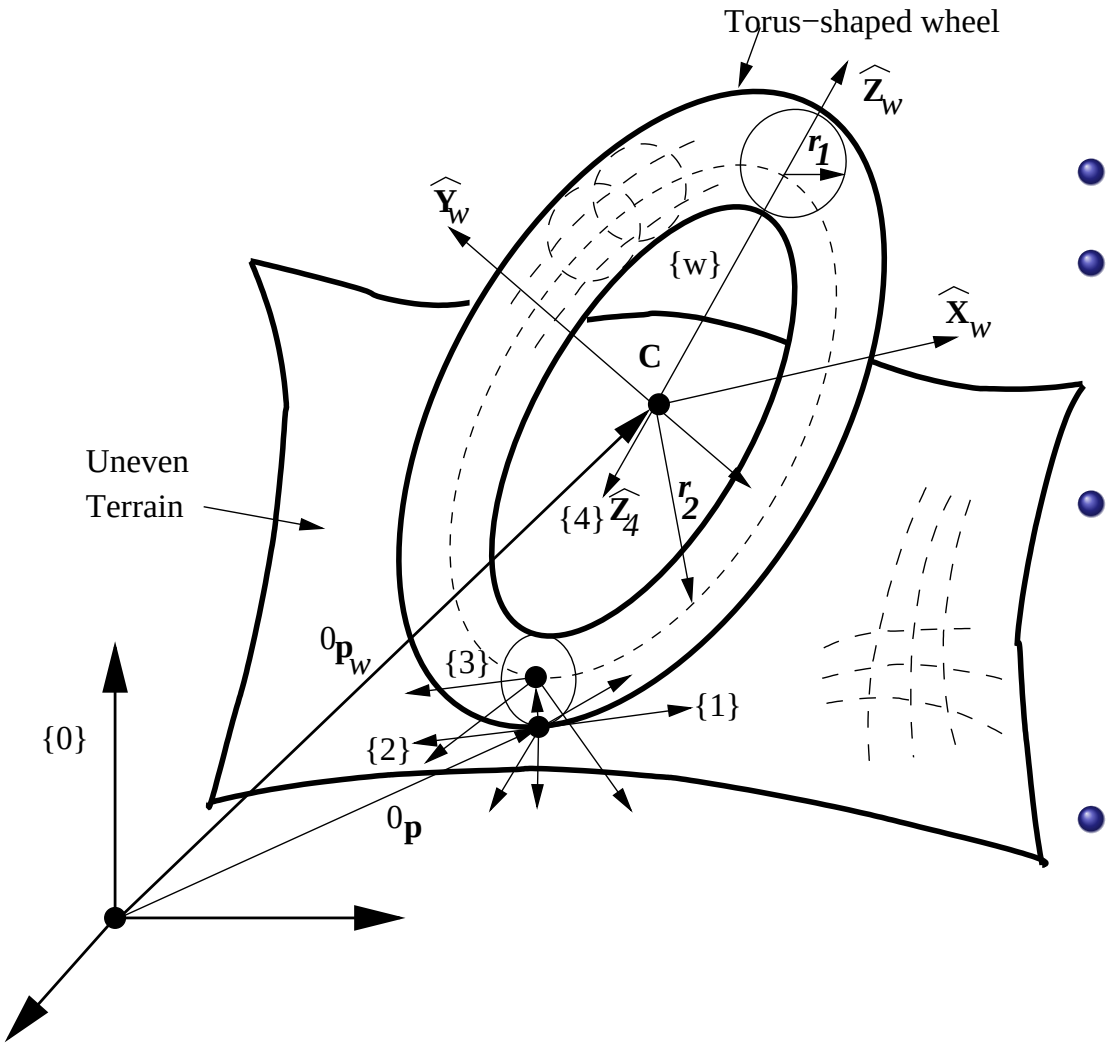
$$
\begin{aligned}
(v_x, v_y)^T &= -[\mathbf{M}_1](\dot{u}_1, \dot{v}_1)^T + [R_\psi][\mathbf{M}_2](\dot{u}_2, \dot{v}_2)^T \\
(\omega_y, -\omega_x)^T &= -[\mathbf{K}_1][\mathbf{M}_1](\dot{u}_1, \dot{v}_1)^T - [R_\psi][\mathbf{K}_2][\mathbf{M}_2](\dot{u}_2, \dot{v}_2)^T \\
\omega_z &= \dot{\psi} - [\mathbf{T}_1][\mathbf{M}_1](\dot{u}_1, \dot{v}_1)^T - [\mathbf{T}_2][\mathbf{M}_2](\dot{u}_2, \dot{v}_2)^T \\
v_z &= 0
\end{aligned}
$$

- $v_z = 0$ *holonomic* constraint $\Rightarrow$ Ensures surfaces stay in contact!
- Five other equations need to be *numerically* integrated with initial conditions for solution.

KINEMATICS OF CONTACT

- Contact equations similar to constraint equations for joints (see Module 2, Lecture 2)
- *Main difference*: equations contain derivatives with respect to time!
- *Two main types of contacts* :
  - *Pure rolling* — $v_x = v_y = 0 \rightarrow$ Important for WMRs.
  - *Pure sliding* — $\omega_x = \omega_y = 0$.
- Pure rolling $v_x = v_y = v_z = 0 \rightarrow$ Three DOF *in velocities*.
- Very much unlike a 3 DOF spherical joint $\rightarrow$ S joint $x = y = z$ are also same for both links!
- Pure rolling — *Non-holonomic* $\rightarrow$ Only $v_x = v_y = 0$ (also $v_z = 0$) and x, y, z coordinates of the contact point can change as the rolling proceeds!

Single Wheel on Uneven Terrain



- $\{C_{r_2}\}$ is same as $\{0\}$.
- $\{C_{r_1}\}$ is fixed at the wheel centre C, same as $\{w\}$.
- $\{C_{l_1}\}$ and $\{C_{l_2}\}$ at the contact point are denoted by $\{2\}$ and $\{1\}$.
- $\{3\}$ and $\{4\}$ as shown in figure.

Figure 20: Single wheel on uneven ground

KINEMATIC ANALYSIS

- 4×4 transformation matrices from assigned frames:

$$ {}^{0}_{1}[T] = \begin{pmatrix} l_1 & m_1 & n_1 & u_g \\ l_2 & m_2 & n_2 & v_g \\ l_3 & m_3 & n_3 & f(u_g, v_g) \\ 0 & 0 & 0 & 1 \end{pmatrix}, \quad {}^{1}_{2}[T] = \begin{pmatrix} \cos\psi & -\sin\psi & 0 & 0 \\ -\sin\psi & -\cos\psi & 0 & 0 \\ 0 & 0 & -1 & 0 \\ 0 & 0 & 0 & 1 \end{pmatrix} $$

$l_i,\ m_i,\ n_i,\ i = 1,2,3$ are the components of $\{\mathbf{f}_u/|\mathbf{f}_u|, \mathbf{n} \times \mathbf{f}_u/|\mathbf{f}_u|, \mathbf{n}\}$.

- Transformation matrices from $\{2\}$ to $\{4\}$ are

$$ {}^{2}_{3}[T] = \begin{pmatrix} \sin u_w & 0 & \cos u_w & 0 \\ 0 & 1 & 0 & 0 \\ -\cos u_w & 0 & \sin u_w & -r_1 \\ 0 & 0 & 0 & 1 \end{pmatrix}, \quad {}^{3}_{4}[T] = \begin{pmatrix} 1 & 0 & 0 & 0 \\ 0 & -\sin v_w & \cos v_w & 0 \\ 0 & -\cos v_w & -\sin v_w & -r_2 \\ 0 & 0 & 0 & 1 \end{pmatrix} $$

- Transformation matrix from $\{4\}$ to $\{w\}$ is

$$ {}^{4}_{w}[T] = \begin{pmatrix} -1 & 0 & 0 & 0 \\ 0 & 1 & 0 & 0 \\ 0 & 0 & -1 & 0 \\ 0 & 0 & 0 & 1 \end{pmatrix} $$

KINEMATIC ANALYSIS

- The transformation matrix from $\{w\}$ to $\{0\}$ is

$$ {}^{0}_{w}[T] = {}^{0}_{1}[T]{}^{1}_{2}[T]{}^{2}_{3}[T]{}^{3}_{4}[T]{}^{4}_{w}[T] $$

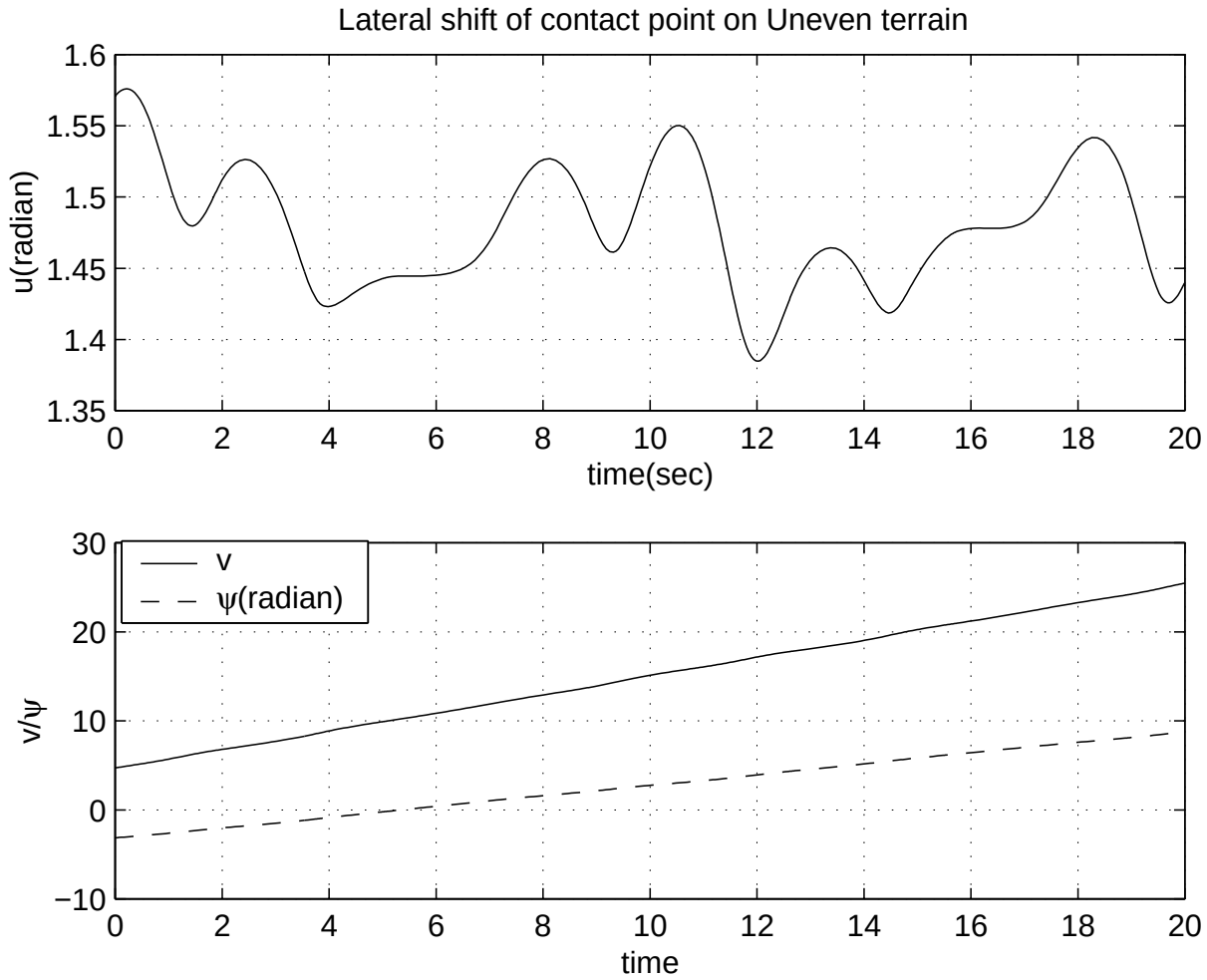
- The contact equation for a single-wheel *rolling without slip*

$$
\begin{aligned}
(\dot{u}_w, \dot{v}_w)^T &= [\mathbf{M}_w]^{-1}([\mathbf{K}_w] + [\mathbf{K}^*])^{-1}[(-\omega_y, \omega_x)^T] \\
(\dot{u}_g, \dot{v}_g)^T &= [\mathbf{M}_g]^{-1}[\mathbf{R}_\psi]([\mathbf{K}_g] + [\mathbf{K}^*])^{-1}[(-\omega_y, \omega_x)^T] \\
\dot{\psi} &= \omega_z + [\mathbf{T}_w][\mathbf{M}_w](\dot{u}_w, \dot{v}_w)^T + [\mathbf{T}_g][\mathbf{M}_g](\dot{u}_g, \dot{v}_g)^T \\
0 &= v_z
\end{aligned}
$$

  w denotes wheel and g denotes ground.

- Inputs: ω_x, ω_y, ω_z.
- Integrate contact equations to obtain evolution of point of contact on wheel *and* ground in time.

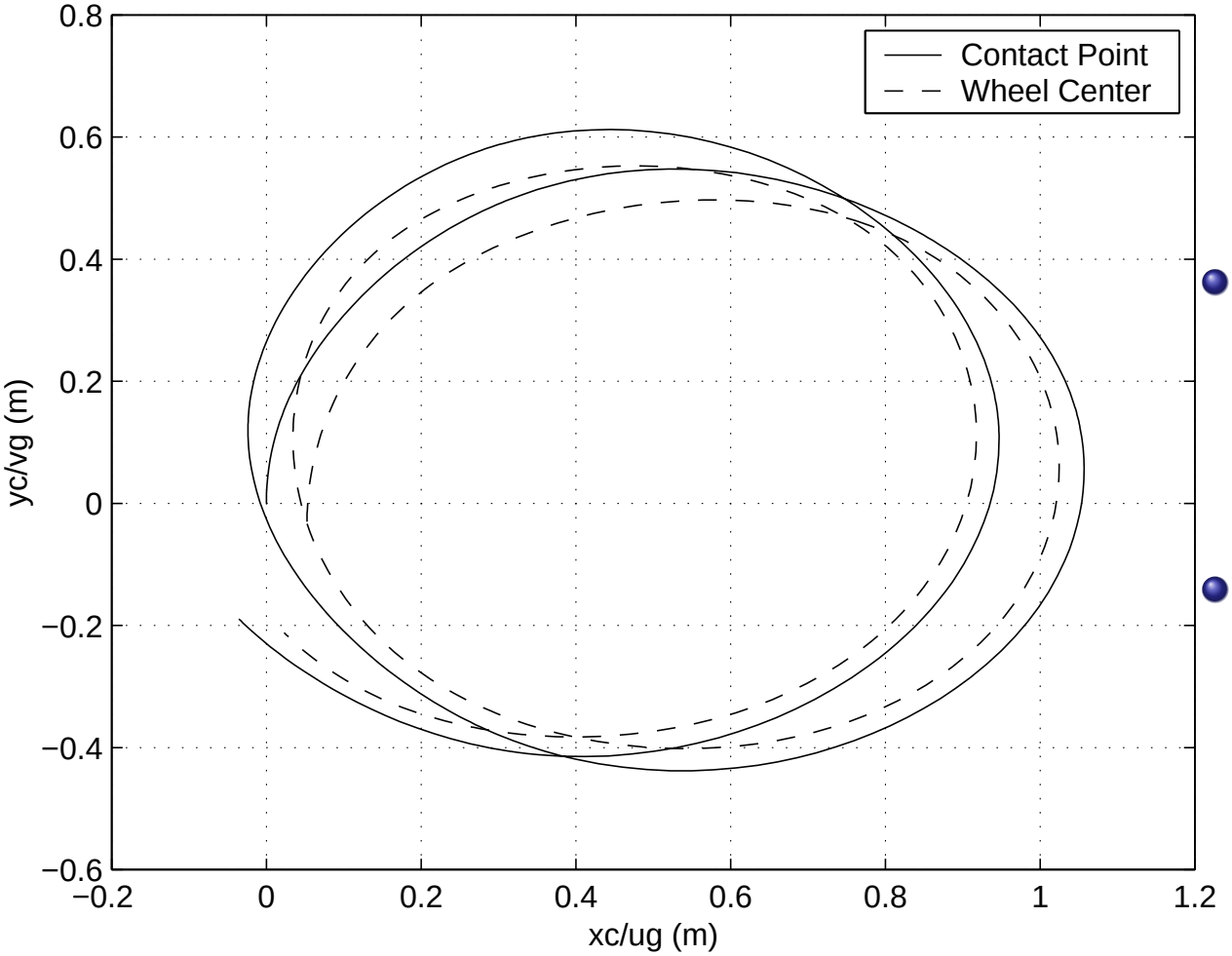
KINEMATIC ANALYSIS



- Simulation for **bi-cubic surface** shown earlier.
- $r_1 = 0.05$ m, $r_2 = 0.25$ m.
- Wheel tilts as it rolls.

Figure 21: Variation of u_w, v_w and ψ with t

KINEMATIC ANALYSIS



- Trace of wheel centre and ground contact point is different.
- Unlike a disk rolling on flat surface.

Figure 22: Plot of wheel centre and ground contact point

Dynamic Analysis

- Equations of motion of a torus-shaped wheel on uneven terrain using Lagrangian formulation.
- Non-holonomic constraints

$$(v_x, v_y)^T = -[\mathbf{M}_w](\dot{u}_w, \dot{v}_w)^T + [R_\psi][\mathbf{M}_g](\dot{u}_g, \dot{v}_g)^T = (0,0)^T$$

after rearranging $[\Psi(\mathbf{q})]\dot{\mathbf{q}} = 0$

- Kinetic energy of wheel
  - Angular velocity ${}^0_w[\Omega]$ from rotation matrix as ${}^0_w[\dot{R}]\ {}^0_w[R]^T$.
  - Linear velocity by differentiating position of wheel centre – ${}^0\mathbf{V}_w = {}^0\dot{\mathbf{p}}_w$
  - Kinetic energy: $KE = \frac{1}{2}\Omega^T[I_w]\Omega + \frac{1}{2}m_w{}^0\mathbf{V}_w{}^2$
- Potential energy: $PE = m_w g z_{wc}$
- Equations of motion (see Module 6, Lecture 1)

$$[\mathbf{M}(\mathbf{q})]\ddot{\mathbf{q}} + [\mathbf{C}(\mathbf{q}, \dot{\mathbf{q}})]\dot{\mathbf{q}} + \mathbf{G}(\mathbf{q}) = \tau + [\Psi(\mathbf{q})]^T\lambda$$

Dynamic Analysis

- Wheel dimensions: $r_1 = 0.05$ m, $r_2 = 0.25$ m.
- Mass of wheel $m_w = 1.0$ kg.
- Inertia components of a torus-shaped wheel

$$[I_w] = \begin{pmatrix} \frac{1}{4} m_w (3{r_1}^2 + 4{r_2}^2) & 0 & 0 \\ 0 & \frac{1}{8} m_w (5{r_1}^2 + 4{r_2}^2) & 0 \\ 0 & 0 & \frac{1}{8} m_w (5{r_1}^2 + 4{r_2}^2) \end{pmatrix}$$

- Initial conditions *satisfy* non-holonomic constrains.
- No external force $\tau = \mathbf{0}$
- Torus-shaped wheels rolls down under gravity on surface shown next.

Dynamic Analysis

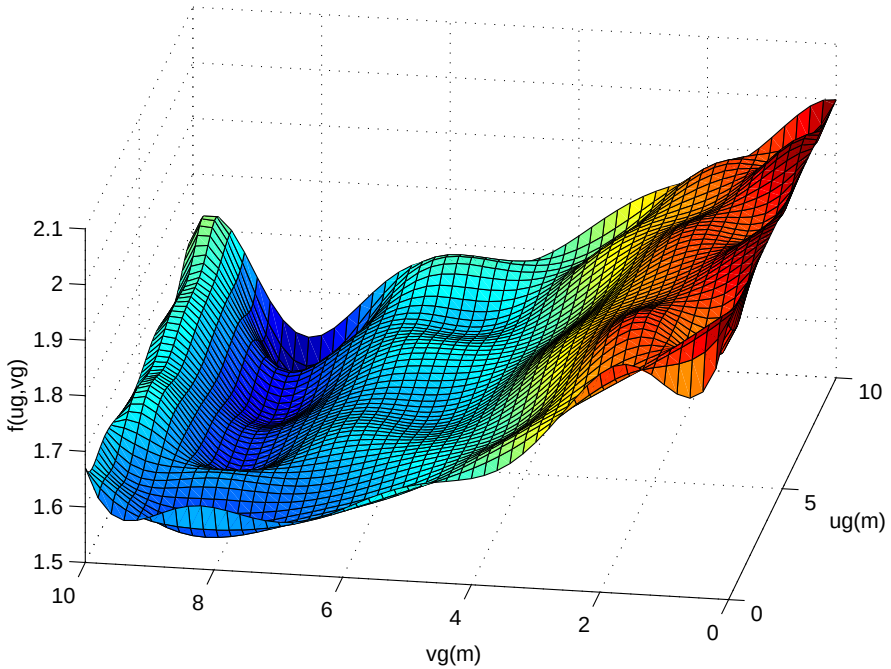


Figure 23: B-spline surface used for single wheel dynamics

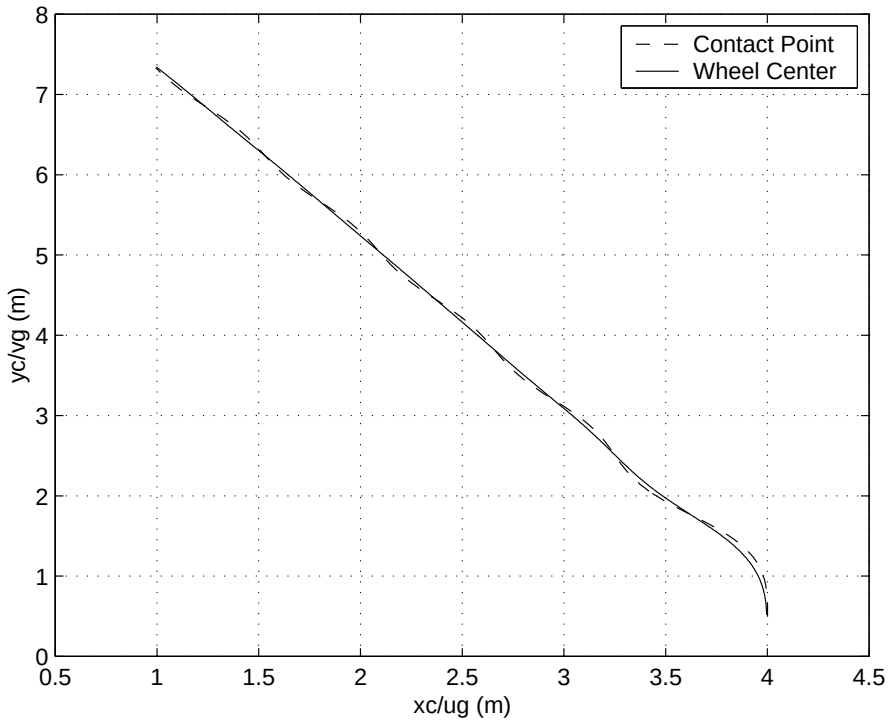


Figure 24: Trace of wheel centre and ground contact points

Dynamic Analysis

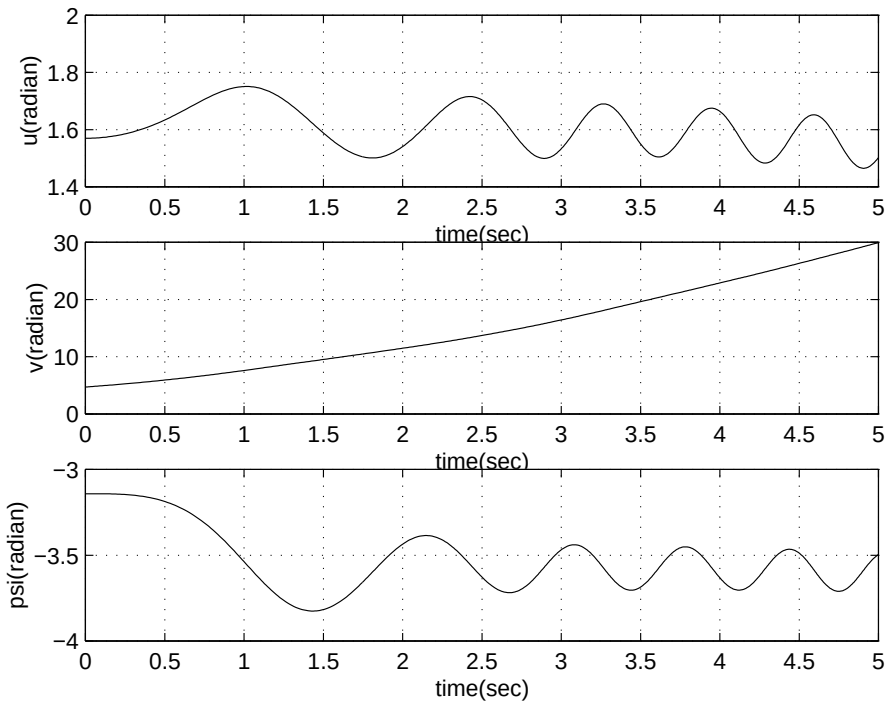


Figure 25: Variation of u_w, v_w and ψ with t

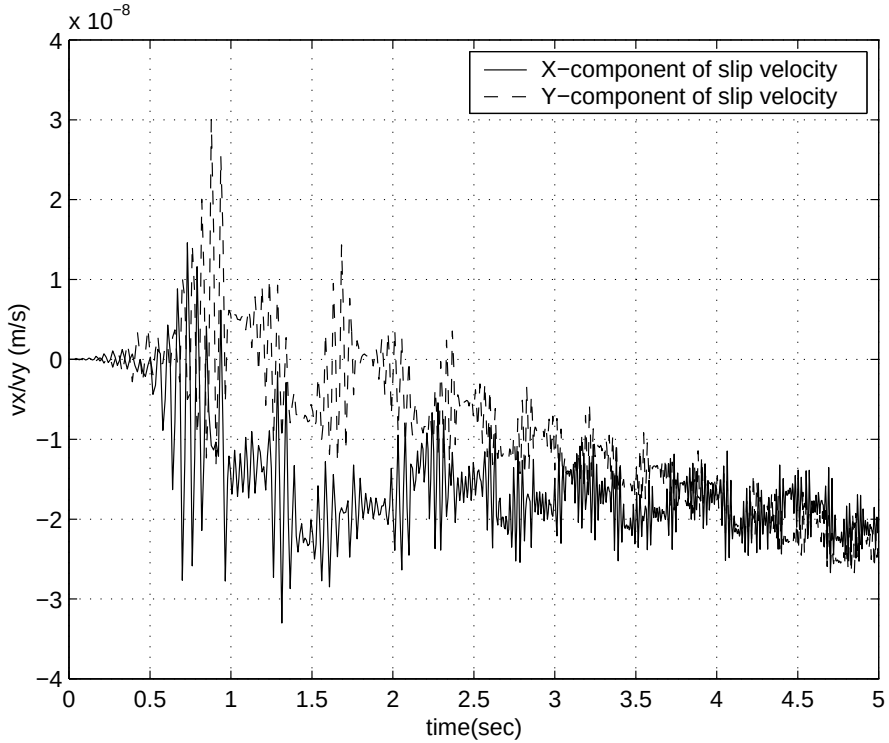


Figure 26: Components of slip velocity at wheel-ground contact point

- Slip components are very small (10^{-8}m/sec).
- Simulation checked for conservation of energy.

A WMR for Traversing Uneven Terrain

- Three torus-shaped wheels connected to rigid platform with rotary (R) joints.
- Two possible configurations – Platform with 3 DOF
  - Each wheel attached to platform with two R joints.
  - For rear wheels — One R joint is actuated by a motor making the wheel roll.
  - For front wheel – One R joint represents steering.
  - For rear wheels – One R joint is passive allowing lateral tilting about axis perpendicular to wheel rotation axis.
  - For front wheel – One R joint represents free rolling of the wheel.
- WMR platform with 6 DOF
  - Each wheel attached to platform by three R joints.
  - 2 R joints in rear and front wheel function as above.
  - Additional R joint in rear wheel allow for steering.
  - Additional R joint in front wheel allow lateral tilt.

3 DOF Configuration

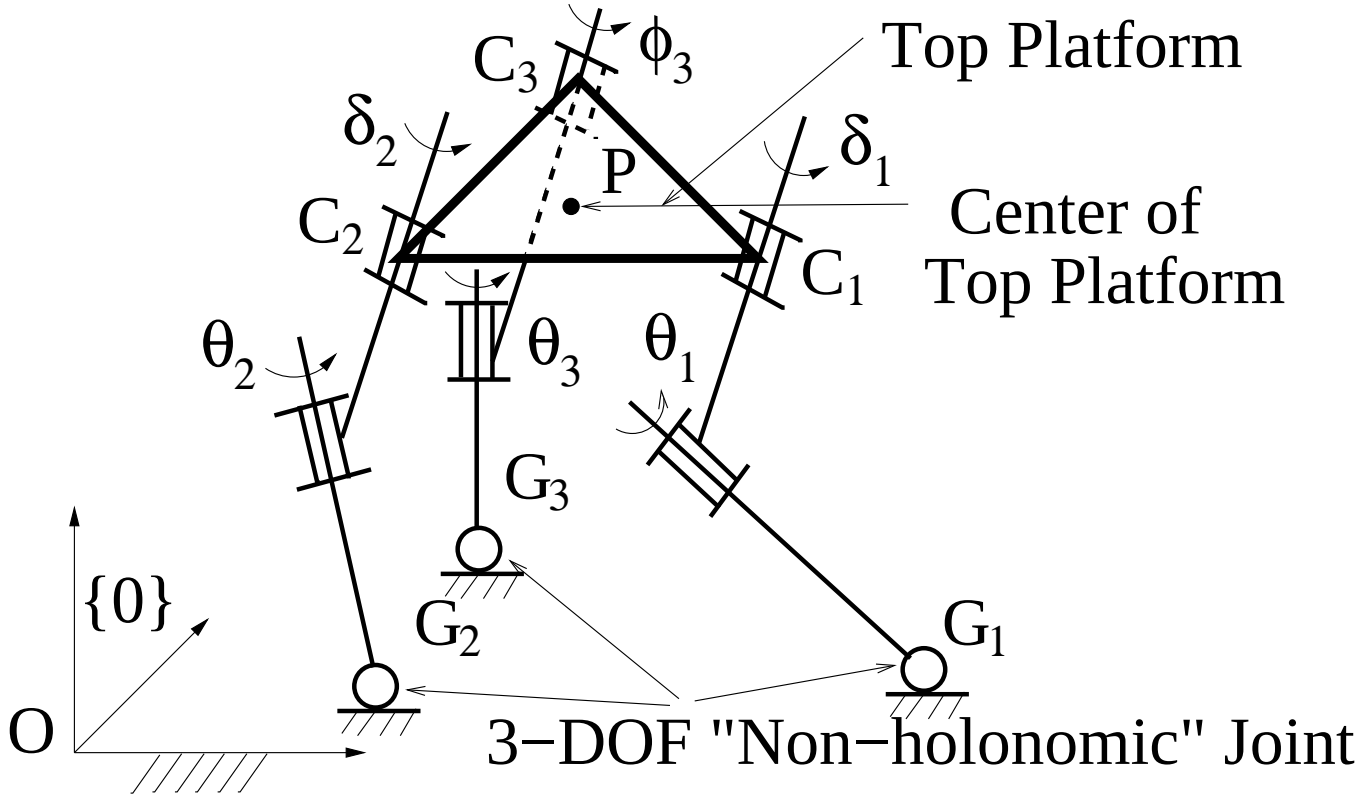


Figure 27: Schematic of a three-wheeled mobile robot with 3 DOF

- Wheel-ground contact has 3 DOF instantaneously – Only velocities are restricted $\rightarrow$ *Non-holonomic joint*.
- Grübler criterion – $\text{DOF} = 6(N-J-1)+\sum_{i=1}^{J} F_i - N = 8$, $J = 9$, and $\sum_{i=1}^{J} F_i = 15 \rightarrow \text{DOF} = 3$.

6 DOF Configuration

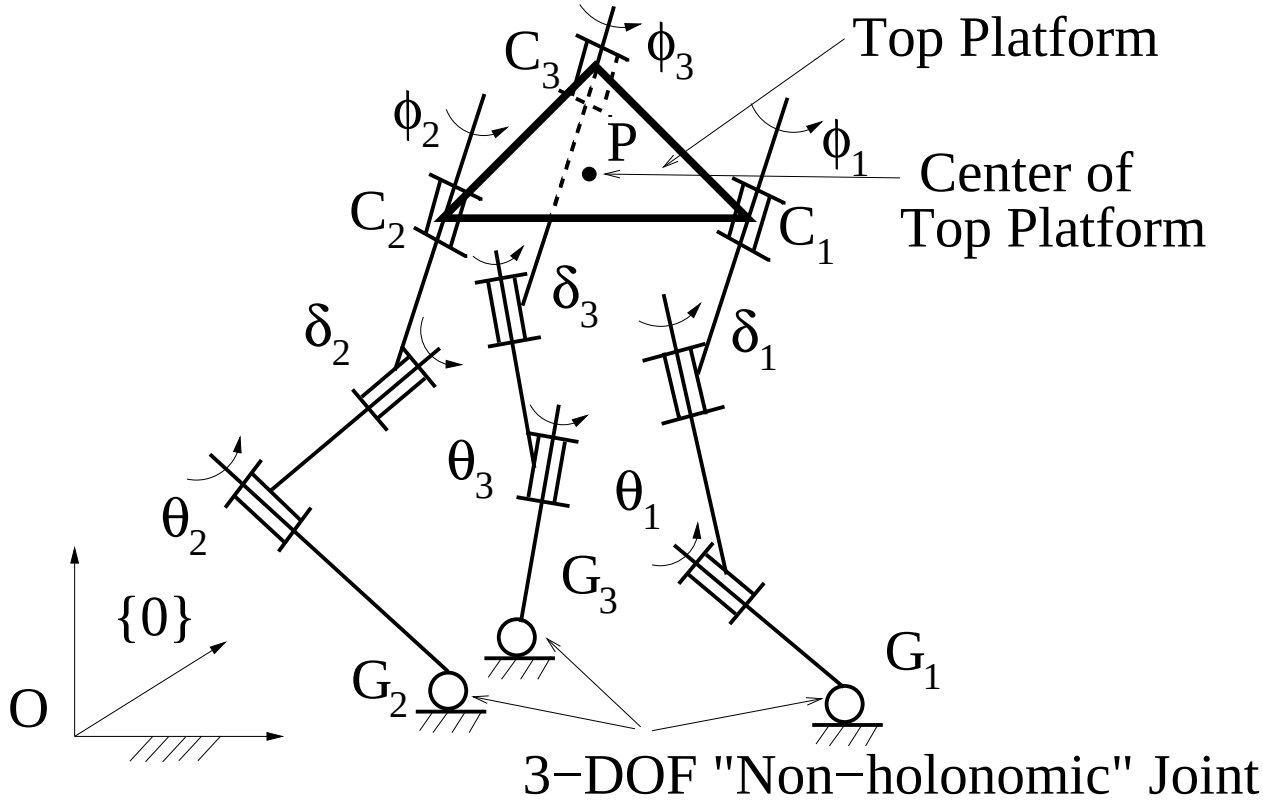


Figure 28: Schematic of three wheeled mobile robot with 6 DOF

- Wheel-ground contact – 3 DOF *non-holonomic joint*.
- Grübler criterion – $\text{DOF} = 6(N - J - 1) + \sum_{i=1}^{J} F_i$, $N = 11$, $J = 12$ and $\sum_{i=1}^{J} F_i = 18 \rightarrow \text{DOF} = 6$.
- Study kinematics and dynamics of 3 DOF configuration.

Summary

- WMR with fixed length axle, moving on uneven terrain, can slip.
- Variable length axle concepts and concept of passive tilting.
- Geometric modeling of torus-shaped wheel and uneven terrain.
- Contact equations representing 5 DOF between two surfaces in single point contact.
- Kinematic and dynamic analysis and simulation of single wheel on uneven terrain.
- Configuration of a three-wheeled mobile robot for traversing uneven terrain without slip.
- Kinematic, dynamic and stability analysis in next lecture.

Outline

1. Contents

2. Lecture 1
   - Wheeled Mobile Robots (WMR) on Flat Terrain

3. Lecture 2*
   - Wheeled Mobile Robots (WMR) on Uneven Terrain

4. Lecture 3*
   - Kinematics and Dynamics of WMR on Uneven Terrain

5. Additional Material
   - Problems, References and Suggested Reading

Contents of Lecture

- Kinematic analysis a three-wheeled mobile robot
  - Solution of the direct kinematics problem.
  - Solution of the inverse kinematics problem.
- Formulation of Equations of Motion for Dynamic analysis.
- Simulation results.
- Stability of three wheeled mobile robot on uneven terrain
- Summary

KINEMATIC ANALYSIS

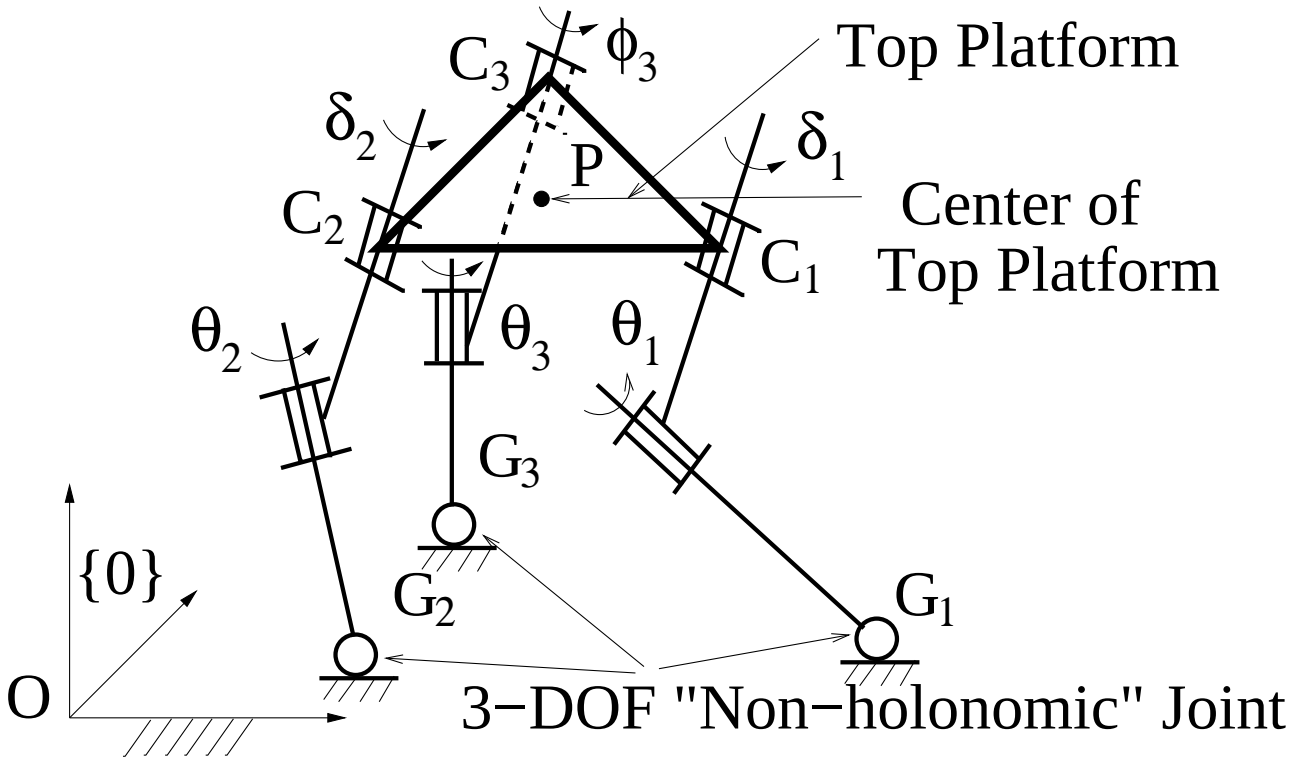


Figure 29: Equivalent instantaneous parallel manipulator

- Instantaneous parallel manipulator with a platform "connected" to ground by three serial chains.
- Actuated: Rear wheel rotations, θ_1 and θ_2, front wheel steering ϕ_3.
- Passive: Rear wheel tilt δ_1, δ_2 and front wheel rotation θ_3.

Kinematic Analysis

- Analyse the WMR as a parallel manipulator at *every* instant.
- *Instantaneously* – Wheels are not fixed as in a parallel manipulator!
- Non-holonomic (no slip) constraints and hence kinematics in terms of joint rates!
- Direct Kinematic: Given actuation rates $\dot{\theta}_1$, $\dot{\theta}_2$ and $\dot{\phi}_3$, the terrain and WMR geometry, find orientation of top platform ${}^0_p[R]$ and the position vector of the centre of the platform.
- Inverse kinematics: Given geometry of WMR and terrain and given any three of $V_{p_x}, V_{p_y}, V_{p_z}, \Omega_{p_x}, \Omega_{p_y}, \Omega_{p_z}$, find rear wheel actuator inputs $\dot{\theta}_1$ and $\dot{\theta}_2$ and the steering input to the front wheel $\dot{\phi}_3$.

KINEMATIC ANALYSIS: ALGORITHM

- *Step 1: Generate the uneven terrain surface:*
  - Use bi-cubic patches or B-splines to reconstruct the surface from elevation data.
  - Find [**M**], [**K**] and [**T**] for the ground and wheels at the three wheel-ground contact points.
- *Step 2: Form contact equations:*
  - For *each* wheel, obtain 5 ODEs in u_i, v_i, u_{g_i}, v_{g_i}, and ψ_i $i = 1, 2, 3$.
  - For no-slip motion, set $v_x = v_y = 0$ for each of the three wheels.
  - ω_x, ω_y, and ω_z are related to Ω_{p_x}, Ω_{p_y}, Ω_{p_z}, and the input and passive joint rates

$$^0(\omega_x, \omega_y, \omega_z)^T = ^0(\Omega_{p_x}, \Omega_{p_y}, \Omega_{p_z})^T + ^0\omega_{\text{input}}$$

  - Above equation *couples* all five sets of ODEs resulting in a set of 15 ODEs in 21 variables – 15 contact variables, $\theta_1, \theta_2, \theta_3$, δ_1, δ_2, and ϕ_3.
  - Out of 21 variables, θ_1, θ_2, and ϕ_3 are actuated and known.

KINEMATIC ANALYSIS: ALGORITHM

- *Step 3: Obtain the angular and linear velocities of centre of the platform:*
  - If γ, β, α be a Z-Y-X Euler angle parametrization (see Module 2, Lecture 1, Slide # 12) representing the orientation of the platform, then

$$^0\Omega_{p_x} = \dot{\alpha}\cos\beta\cos\gamma - \dot{\beta}\sin\gamma = f_1(u_i, v_i, u_{g_i}, v_{g_i}, \psi_i, \dot{u}_i, \dot{v}_i, \dot{u}_{g_i}, \dot{v}_{g_i}, \dot{\psi}_i)$$

$$^0\Omega_{p_y} = \dot{\alpha}\cos\beta\sin\gamma + \dot{\beta}\cos\gamma = f_2(u_i, v_i, u_{g_i}, v_{g_i}, \psi_i, \dot{u}_i, \dot{v}_i, \dot{u}_{g_i}, \dot{v}_{g_i}, \dot{\psi}_i)$$

$$^0\Omega_{p_z} = \dot{\gamma} - \dot{\alpha}\sin\beta = f_3(u_i, v_i, u_{g_i}, v_{g_i}, \psi_i, \dot{u}_i, \dot{v}_i, \dot{u}_{g_i}, \dot{v}_{g_i}, \dot{\psi}_i), \quad i = 1,2,3$$

  - If x_c, y_c, and z_c denote the coordinates of the centre of the platform in $\{0\}$, the linear velocity of the centre of the platform is

$$^0(V_{p_x}, V_{p_y}, V_{p_z})^T \stackrel{\Delta}{=} {}^0(\dot{x}_c, \dot{y}_c, \dot{z}_c)^T = {}^0\mathbf{V}_{w_i} + {}^0(\Omega_{p_x}, \Omega_{p_y}, \Omega_{p_z})^T \times {}^0\mathbf{p}_{c_i}$$

$i = 1,2,3$ denote three wheels, ${}^0\mathbf{p}_{c_i}$ locates the point of attachment of the wheel to the platform from the centre of the platform, and ${}^0\mathbf{V}_{w_i}$ is the velocity of the centre of the wheel.

KINEMATIC ANALYSIS: ALGORITHM

- *Step 4: Form holonomic constraint equations:*
  - Distance between the three points C_1, C_2, and C_3 must remain constant for the moving platform to be *rigid*.
  - *Holonomic* constraint are

$$\begin{aligned} \|{}^0\mathbf{p}_{C_1} - {}^0\mathbf{p}_{C_2}\|^2 &= l_{12}^2 \\ \|{}^0\mathbf{p}_{C_2} - {}^0\mathbf{p}_{C_3}\|^2 &= l_{23}^2 \\ \|{}^0\mathbf{p}_{C_3} - {}^0\mathbf{p}_{C_1}\|^2 &= l_{31}^2 \end{aligned}$$

    ${}^0\mathbf{p}_{C_i}$, $i = 1,2,3$ locate C_1, C_2, C_3, from the origin of $\{0\}$ and l_{ij} is the distance between centres of wheels i and j, respectively.
  - Holonomic constraints are same as spherical-spherical pair (S-S) joint constraint of Module 2, Lecture 2, Slide # 34.

KINEMATIC ANALYSIS: ALGORITHM

- *Solution of Direct Kinematics Problem:*
  - Steps 1, 2 & 4: 15 ODEs, 3 algebraic equations in 21 variables.
  - 18 Unknown variables – $\dot{\theta}_1$, $\dot{\theta}_2$ and $\dot{\phi}_3$ are given!
  - Differentiate holonomic constraints $\rightarrow$ Convert to a system of 18 ODEs.
  - Integrate using ODE solver with initial conditions.
  - Obtain position vector of centre and orientation of platform from 21 variables at each t
- *Solution of Inverse Kinematics Problem:*
  - Steps 1 to 4: 21 ODEs, 3 algebraic equations.
  - Assuming linear velocity of the platform $\dot{x}_c$, $\dot{y}_c$, angular velocity about vertical, $\dot{\gamma}$, are given $\rightarrow$ 24 unknowns.
  - Convert DAE's to ODEs.
  - Integrate set of 24 ODEs and obtain required θ_1, θ_2 and ϕ_3 as function of t.
- *Initial conditions* for the direct and inverse kinematics problems *must* satisfy the *holonomic and non-holonomic* constraints.

Numerical simulations results for direct kinematics

- Geometry of the WMR
  - Length of the rear axle 1 m.
  - Distance of the centre of front wheel from middle of the rear axle 1 m.
  - Torus-shaped wheel: $r_1 = 0.05$ m, $r_2 = 0.25$ m.
  - WMR centre is at the centroid of the triangular platform.
- Initial conditions: $u_1 = 1.5816$, $v_1 = \frac{3\pi}{2}$, $u_{g_1} = 4.089$ m, $v_{g_1} = 0.3917$ m, $\psi_1 = -3.1414$, $u_2 = 1.5560$, $v_2 = \frac{3\pi}{2}$, $u_{g_2} = 3.1$ m, $v_{g_2} = 0.4$ m, $\psi_2 = -3.1413$, $u_3 = 1.5735$, $v_3 = \frac{3\pi}{2}$, $u_{g_3} = 3.5977$ m, $v_{g_3} = 1.4097$ m, $\psi_3 = -3.1404$, $\theta_3 = 0$, $\delta_1 = 0$, and $\delta_2 = 0$ — All angles in radians. Initial conditions *satisfy* constraints.
- Actuator inputs: $\dot{\theta}_1 = -1$ rad/sec, $\dot{\theta}_2 = -0.9$ rad/sec, $\dot{\phi}_3 = 0.005t$ rad/sec.
- Uneven surface same as used for single wheel dynamic simulation.

Numerical simulations results for direct kinematics

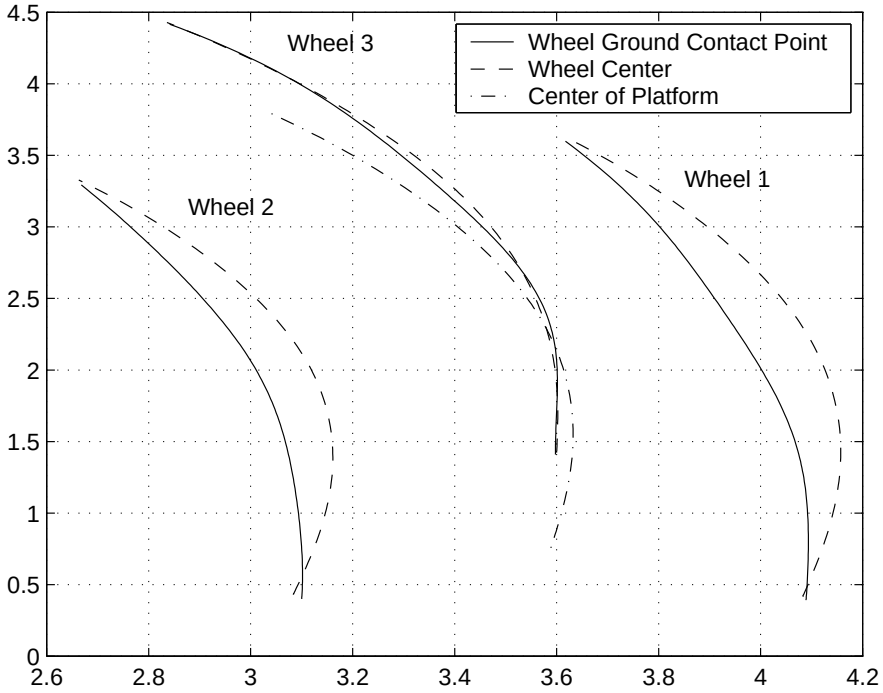


Figure 30: Locus of wheel-ground contact point, wheel centre and platform centre

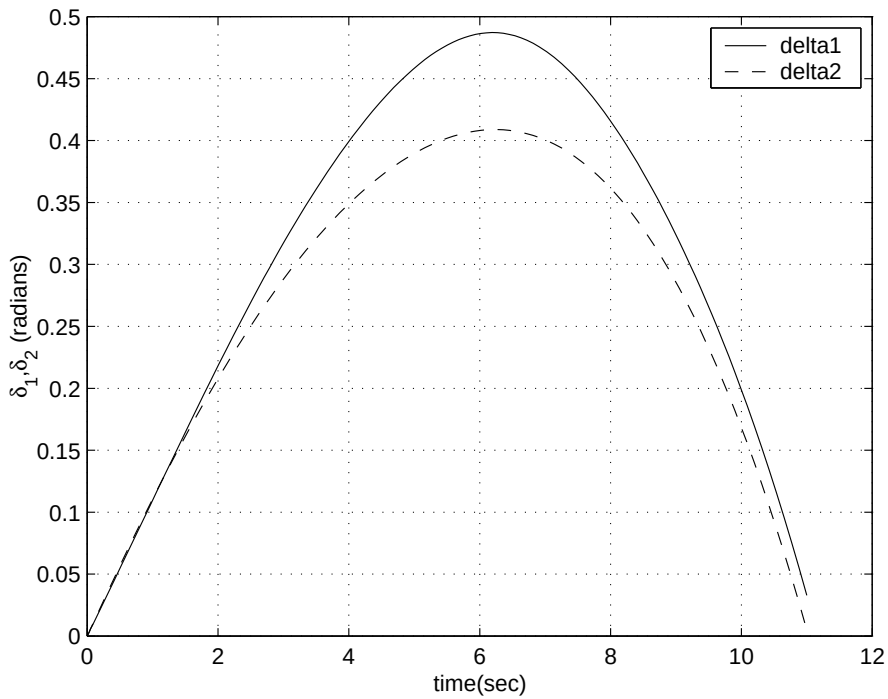


Figure 31: Variation of lateral tilt δ_1 and δ_2

- The locus of wheel centres *not* same as wheel-ground contact point – Uneven terrain and lateral tilt!
- Lateral tilt changes at different points of the uneven terrain.

Numerical simulations results for direct kinematics

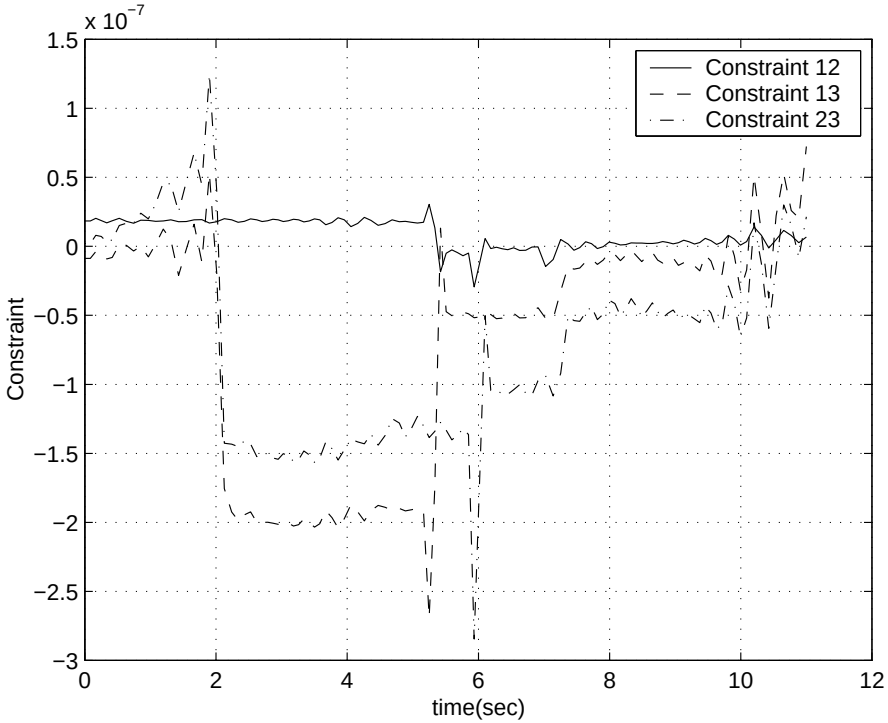


Figure 32: Satisfaction of holonomic constraints

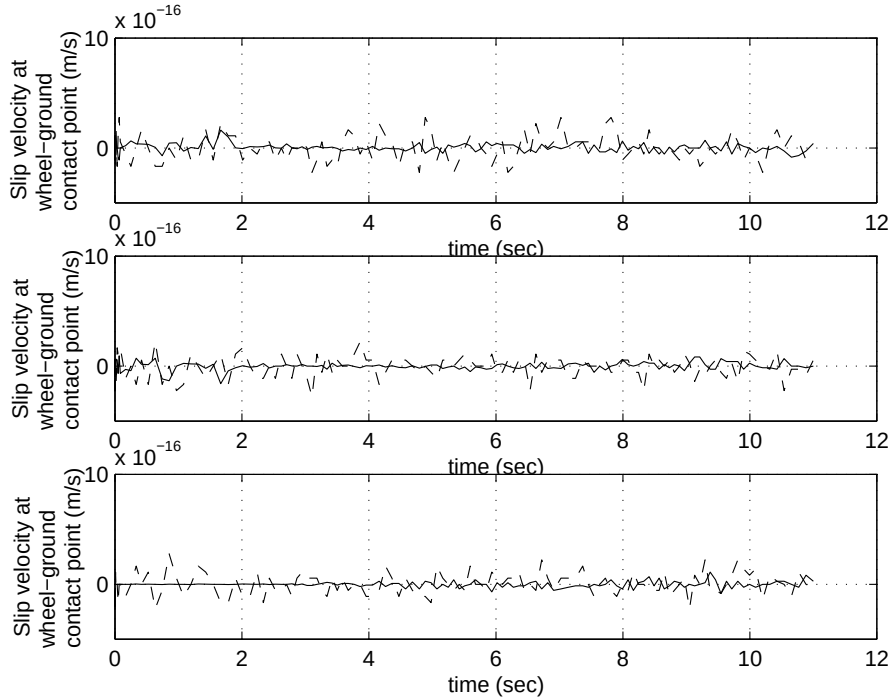


Figure 33: Slip velocities at wheel-ground contact points for three wheels

- The holonomic constraints are satisfied up to 10^{-7} m
- There is virtually no slip – WMR traverses uneven terrain without slip!!

Numerical simulations results for direct kinematics

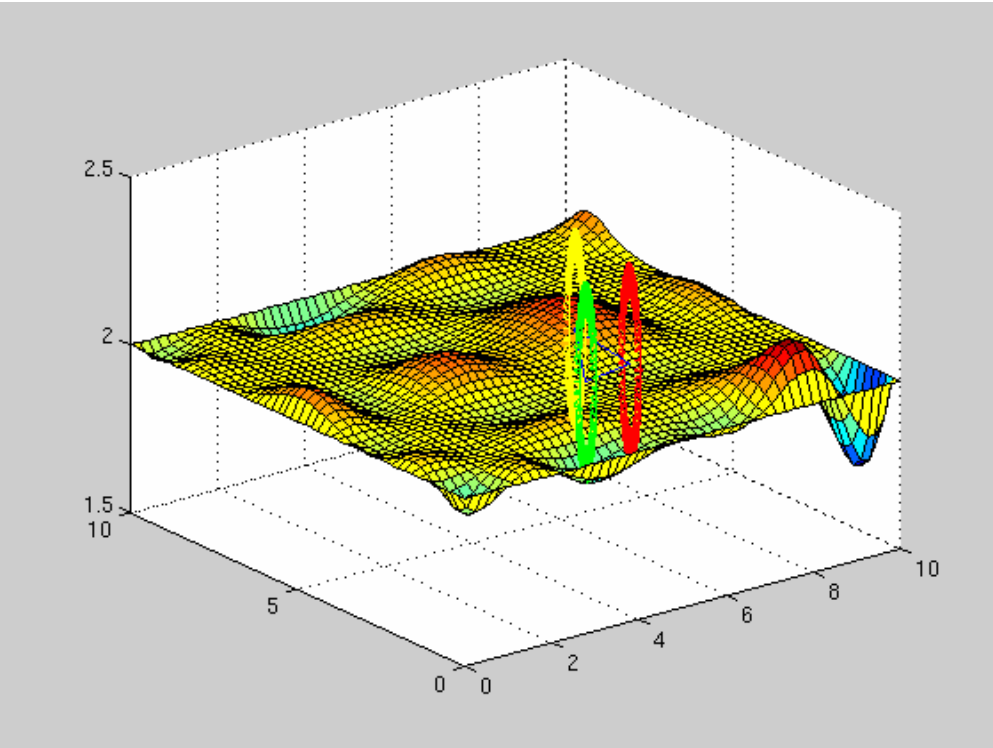


Figure 34: Video of direct kinematics of WMR

See video[4] for a simulation of the three wheeled mobile robot on uneven terrain.

[4] Copy and paste link in a *New Window/Tab* by *right click*. Close *New Window/Tab* after viewing.

Numerical simulations results for inverse kinematics

- Geometry of the WMR – Same as used in direct kinematics
  - Length of the rear axle 1 m.
  - Distance of the centre of front wheel from middle of the rear axle 1 m.
  - Torus-shaped wheel: $r_1 = 0.05$ m, $r_2 = 0.25$ m.
  - WMR centre is at the centroid of the triangular platform.
- Initial conditions: $u_1 = 1.5801$, $v_1 = \frac{3\pi}{2}$, $u_{g_1} = 3.9904$ m, $v_{g_1} = 0.4895$ m, $\psi_1 = -3.1415$, $u_2 = 1.5535$, $v_2 = \frac{3\pi}{2}$, $u_{g_2} = 2$ m, $v_{g_2} = 0.5$ m, $\psi_2 = -3.1411$, $u_3 = 1.5808$, $v_3 = \frac{3\pi}{2}$, $u_{g_3} = 3.4898$ m, $v_{g_3} = 1.5702$ m, $\psi_3 = -3.1414$, $z_c = 2.22$ m, $\alpha = -0.0448$, and $\beta = -0.0498$ — All angles in radians. Initial conditions *satisfy* constraints.
- Given inputs: $\dot{x}_c = 0.03$ m/sec, $\dot{y}_c = 0.15$ m/sec, and $\dot{\gamma} = -0.005t$ rad/sec.
- Uneven surface same as used for direct kinematics.

Numerical simulations results for inverse kinematics

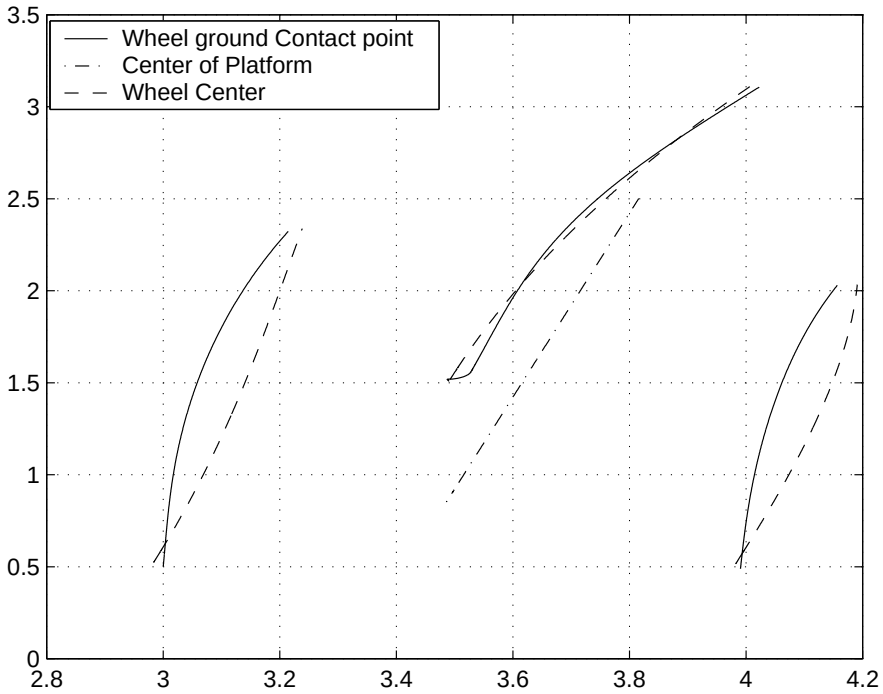


Figure 35: Locus of wheel-ground contact point, wheel centre and platform centre

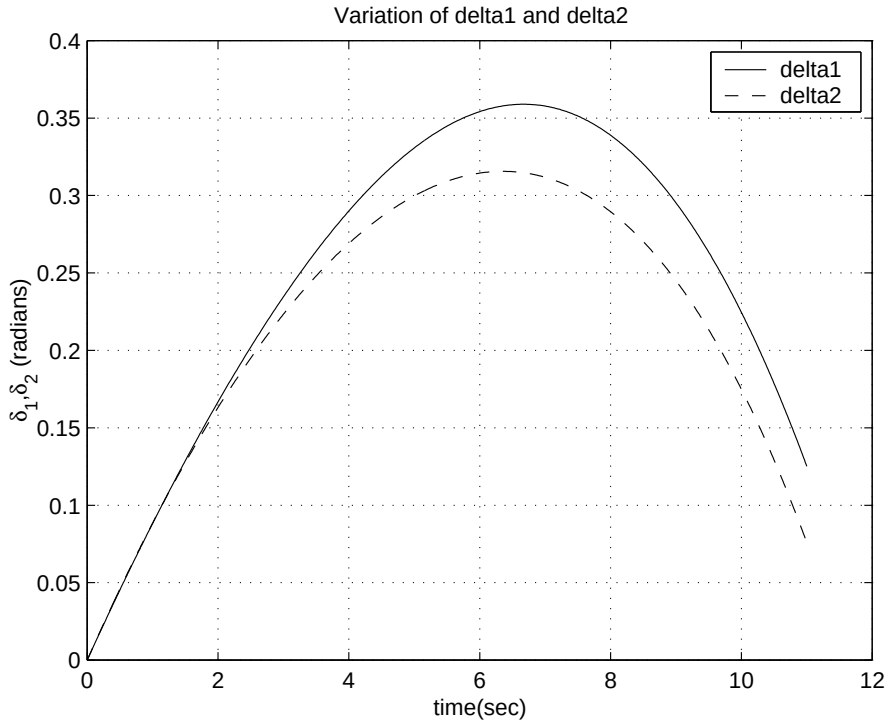


Figure 36: Variation of lateral tilt δ_1 and δ_2

- Due to uneven terrain, locus of wheel centres are *not* same as wheel-ground contact point.
- Lateral tilt changes at different points of uneven terrain.

Numerical simulations results for direct kinematics

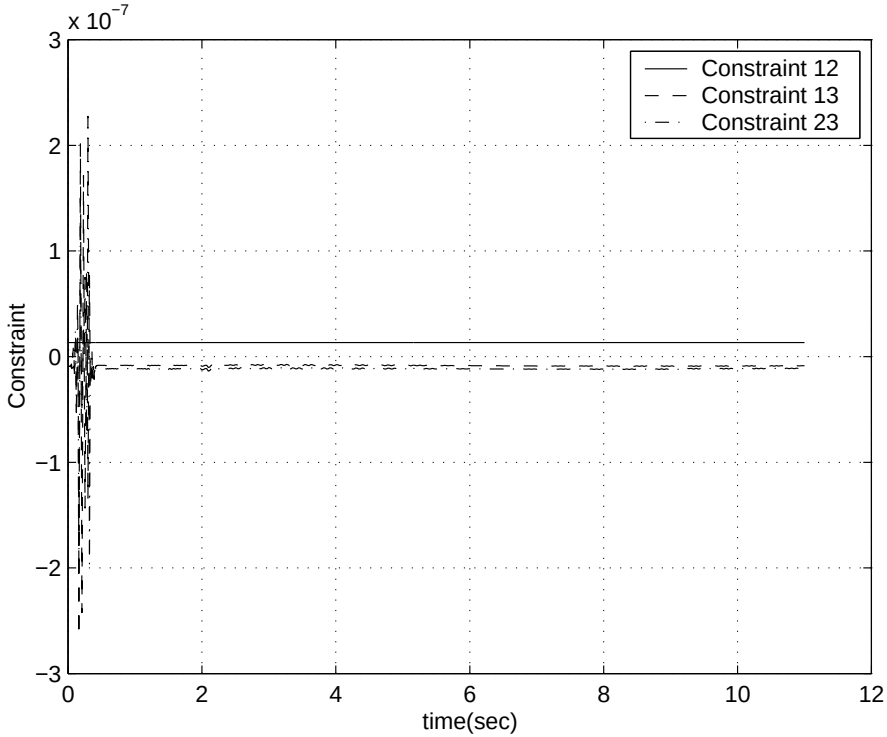


Figure 37: Satisfaction of holonomic constraints

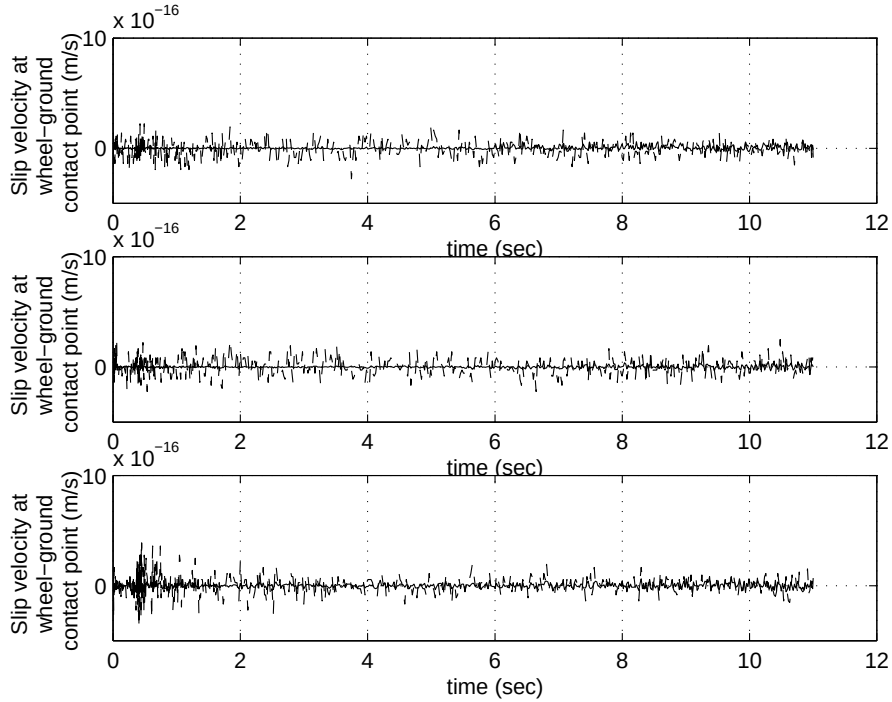


Figure 38: Slip velocities at wheel-ground contact points for three wheels

- The holonomic constraints are satisfied up to 10^{-7} m
- There is virtually no slip – WMR traverses uneven terrain without slip!!

Dynamic Analysis

- Formulation of equation of motion for WMR using Lagrangian formulation.
  - Kinetic energy of wheels, platform and 'links' connecting actuated and passive joints to platform.
  - Potential energy due to gravity.
- 15 contact variables at three wheel-ground contact points, 3 passive, 3 actuated and 6 variables for position and orientation of WMR platform $\rightarrow$ Total 27 generalised coordinates.
- Three actuating torques, two in rear wheel and for front wheel steering.
- Need 24 independent constraint equations for the system to be well-posed – Inverse kinematics equations!!
- Derive equations of motion subjected to holonomic and non-holonomic constraints (see Module 6, Lecture 1).

LAGRANGIAN FORMULATION

- Total kinetic energy

$$KE = (KE)_{w_1} + (KE)_{w_2} + (KE)_{w_3} + (KE)_{\text{platform}} + (KE)_{\text{actuators}} + (KE)_{\text{links}}$$

- Total potential energy

$$PE = (PE)_{w_1} + (PE)_{w_2} + (PE)_{w_3} + (PE)_{\text{platform}} + (PE)_{\text{actuators}} + (PE)_{\text{links}}$$

- All kinetic energy and potential energy components can be found (see Chakraborty & Ghosal, 2005).
- Constraints equation from inverse kinematics: $[\Psi]\dot{\mathbf{q}} = 0$ – $[\Psi]$ is a 24×27 matrix.
- Equations of motion from Lagrangian formulation

$$[\mathbf{M}(\mathbf{q})]\ddot{\mathbf{q}} + [\mathbf{C}(\mathbf{q}, \dot{\mathbf{q}})]\dot{\mathbf{q}} + \mathbf{G}(\mathbf{q}) = \tau + [\Psi(\mathbf{q})]^T \lambda$$

  $[\mathbf{M}(\mathbf{q})]$ is a 27×27 mass matrix, $[\mathbf{C}(\mathbf{q}, \dot{\mathbf{q}})]\dot{\mathbf{q}}$, $\mathbf{G}(\mathbf{q})$ and τ are 27×1 vectors.
- *Only* three elements of τ, corresponding to θ_1, θ_2, ϕ_3, are non-zero.

LAGRANGIAN FORMULATION

- λ is 24×1 vector of the Lagrange multipliers.
- Solve for λ as shown in (see Module 6, Lecture 1, Slide # 17).
- Finally obtain a set of 27 second-order ODEs – Obtained in symbolic form by using Mathematica® extensively!
- With actuators locked and wheels tilted, WMR falls under own weight! – Contrary to a normal parallel manipulator !!
- Wheel-ground contact modeled as *instantaneous* 3 DOF joint – *Not* like a spherical (S) joint.
- *Form closure* not present $\rightarrow$ Additional terms modeling a torsion springs and a damper (preventing falling under own weight with actuators locked) is added in τ corresponding to lateral tilts

$$k_{s_i}\delta_i + k_{d_i}\dot{\delta}_i, \quad (i = 1, 2)$$

k_{s_i} and k_{d_i} are spring constant and damping.

Dynamic Analysis: Algorithm

- *Step 1: Generate the uneven terrain surface*
  - Reconstruct the surface from elevation data.
  - Derivative of constraints are required $\rightarrow \mathscr{C}^3$ continuity required.
  - Fourth degree B-spline surface using MATLAB® Spline Tool Box.
- *Step 2: Form equations of motion* – 27 second-order ODEs.
- *Step 3: Obtain initial conditions*
  - Initial conditions must satisfy no-slip and holonomic constraints.
  - 3 actuated variables can be chosen arbitrarily.
  - Rest 24 obtained using inverse kinematics equations.
- *Step 4: Solve ODEs numerically* – ODE solver in MATLAB® used to obtain evolution of all generalised coordinates.

NUMERICAL SIMULATIONS RESULTS

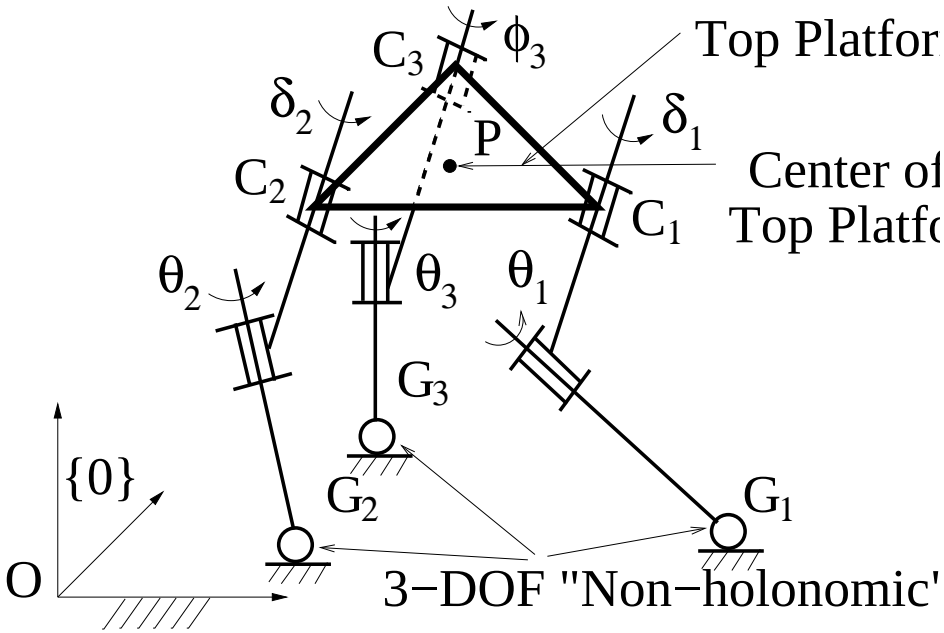


Figure 39: Schematic of the 3 DOF WMR

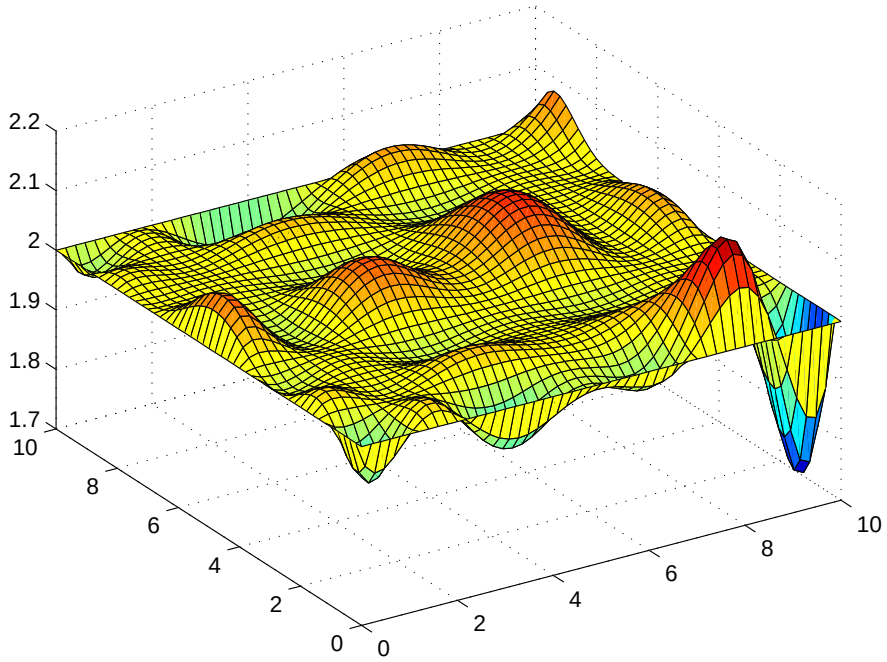


Figure 40: B-spline surface with $\mathscr{C}^3$ continuity

- Synthetic elevation data
- Uneven terrain generated using MATLAB® Spline Tool Box

NUMERICAL SIMULATIONS RESULTS

- Mass of platform = 10 kg, Mass of each wheel = 1 Kg.
- Maximum allowable deflection of δ_i is $\pi/4$ under self-weight $\Rightarrow$ $k_{s_i} = 16.24$ N-m/rad and $k_{d_i} = 0.57$ N-m-s/rad.
- Initial conditions: $u_1 = 1.57$, $v_1 = \frac{3\pi}{2}$, $u_{g_1} = 5.008$ m, $v_{g_1} = 1.5067$ m, $\psi_1 = -3.142$, $u_2 = 1.5648$, $v_2 = \frac{3\pi}{2}$, $u_{g_2} = 4$ m, $v_{g_2} = 1.5$ m, $\psi_2 = -3.1418$, $u_3 = 1.5818$, $v_3 = \frac{3\pi}{2}$, $u_{g_3} = 4.4897$ m, $v_{g_3} = 2.483$ m, $\psi_3 = -3.1419$, $\theta_1 = 0$, $\theta_2 = 0$, $\theta_3 = 0$, $\delta_1 = 0$, $\delta_2 = 0$, $\phi_3 = 0$, $z_c = 2.3088$ m, $\alpha = -0.0127$, and $\beta = 0.0133$ – All angles in radians.
- All the initial values of the first derivatives are chosen to be 0.
- Inputs: $\tau_1 = -0.35$ N-m, $\tau_2 = -0.5$ N-m, and $\tau_3 = -0.001t$ N-m.

NUMERICAL SIMULATIONS RESULTS

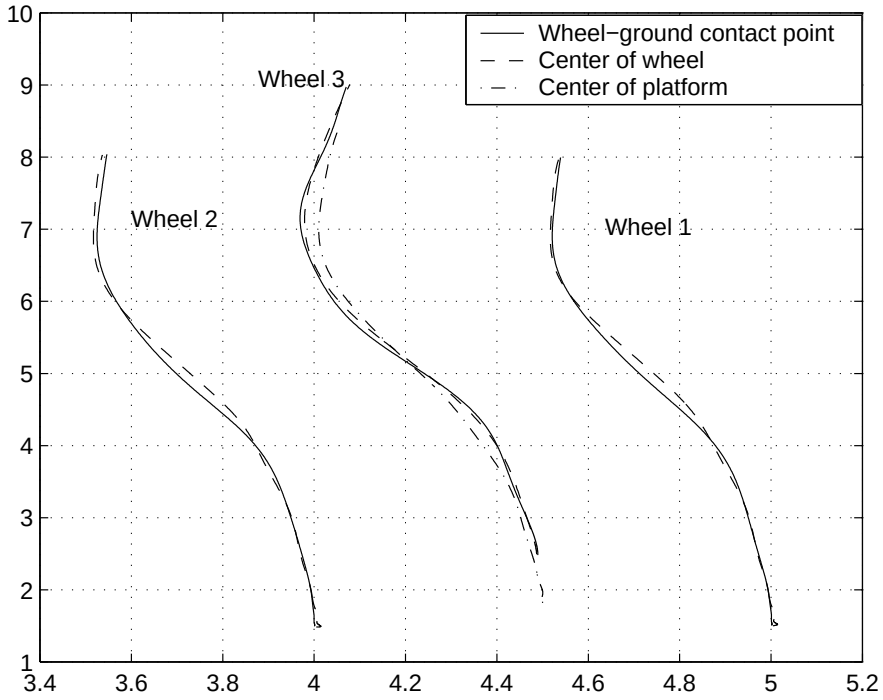


Figure 41: Locus of wheel-ground contact point, wheel centre and platform centre

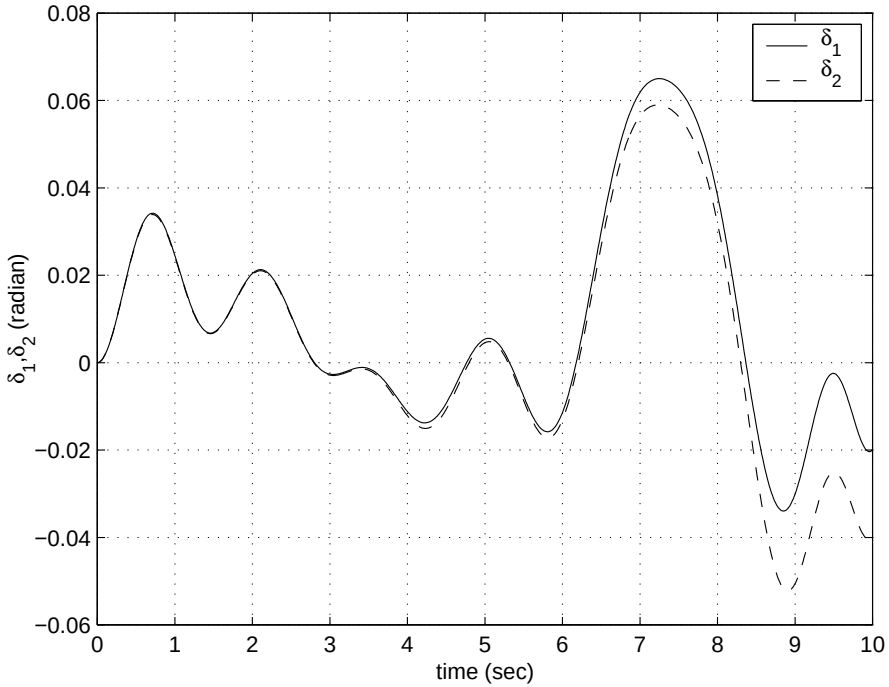


Figure 42: Variation of δ_1 and δ_2

- Uneven terrain – δ_1 and δ_2 varies automatically to avoid slip.

NUMERICAL SIMULATIONS RESULTS

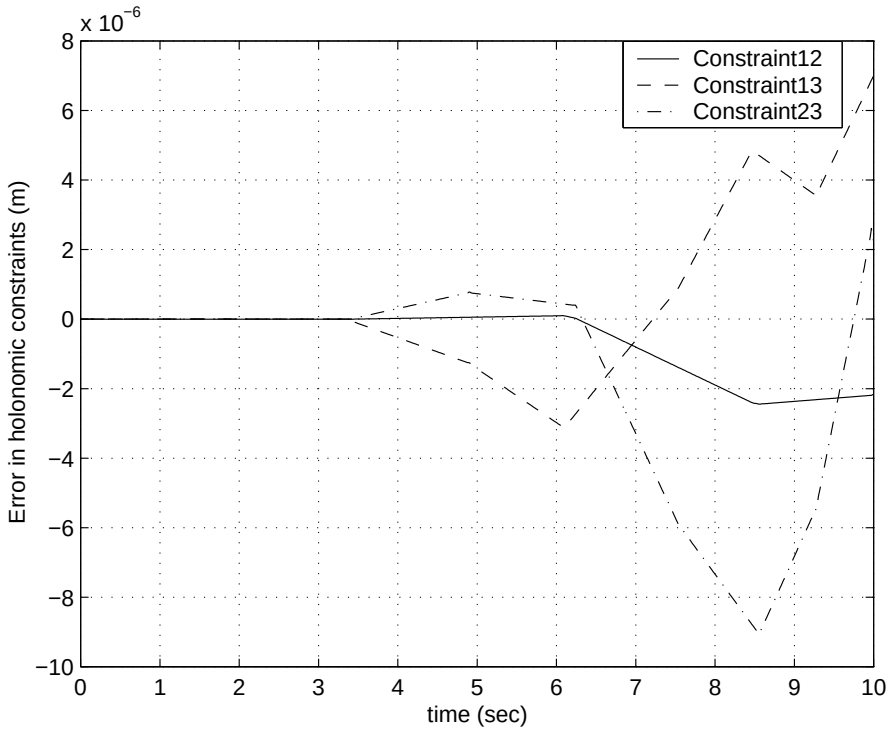


Figure 43: Satisfaction of holonomic constraints in dynamics

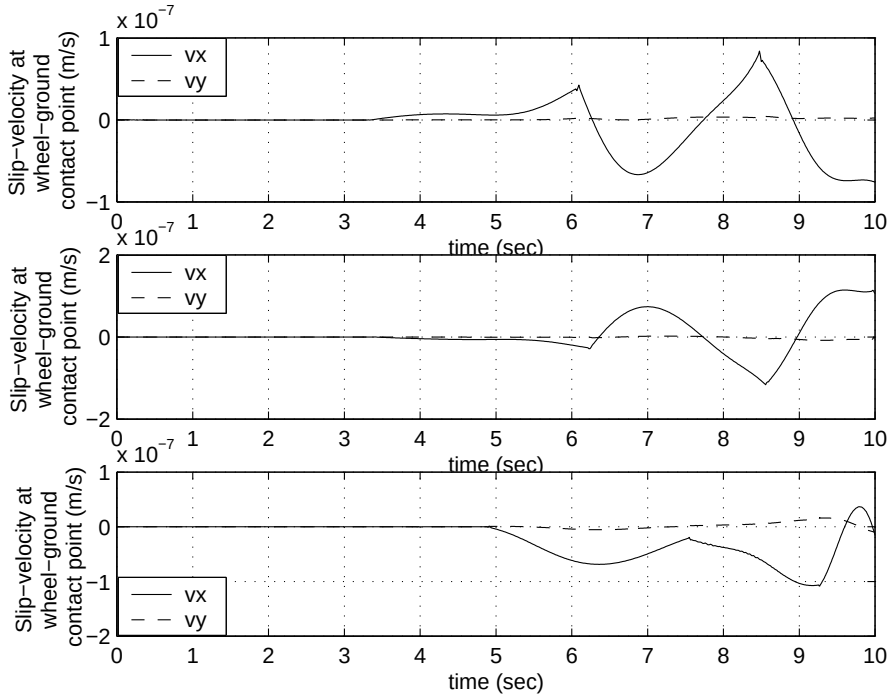


Figure 44: Slip velocities at wheel-ground contact points for three wheels

- All constraints are satisfied at least up to 10^{-7} m.
- Three-wheeled mobile robot can traverses uneven terrain without slip!!

Stability Analysis

- Uneven terrain – Loss of vehicle stability due to tip-over or roll over.
- Tip-over – Vehicle undergoes rotation resulting in reduction in number of vehicle-ground contact points.
- Mobility is lost and, if rotational motion is not arrested, vehicle overturns.
- Need a 'measure' of stability to warn operator.
- Placement of centre of mass, speed, acceleration, external forces/moments and nature of terrain determine tip-over or stability.
- Various measures of stability – Force-angle stability measure (Papadopoulos and Rey, 1996) used.
- Investigate stability of the earlier studied three-wheeled mobile robots with torus-shaped wheels for different conditions.

FORCE-ANGLE STABILITY MEASURE

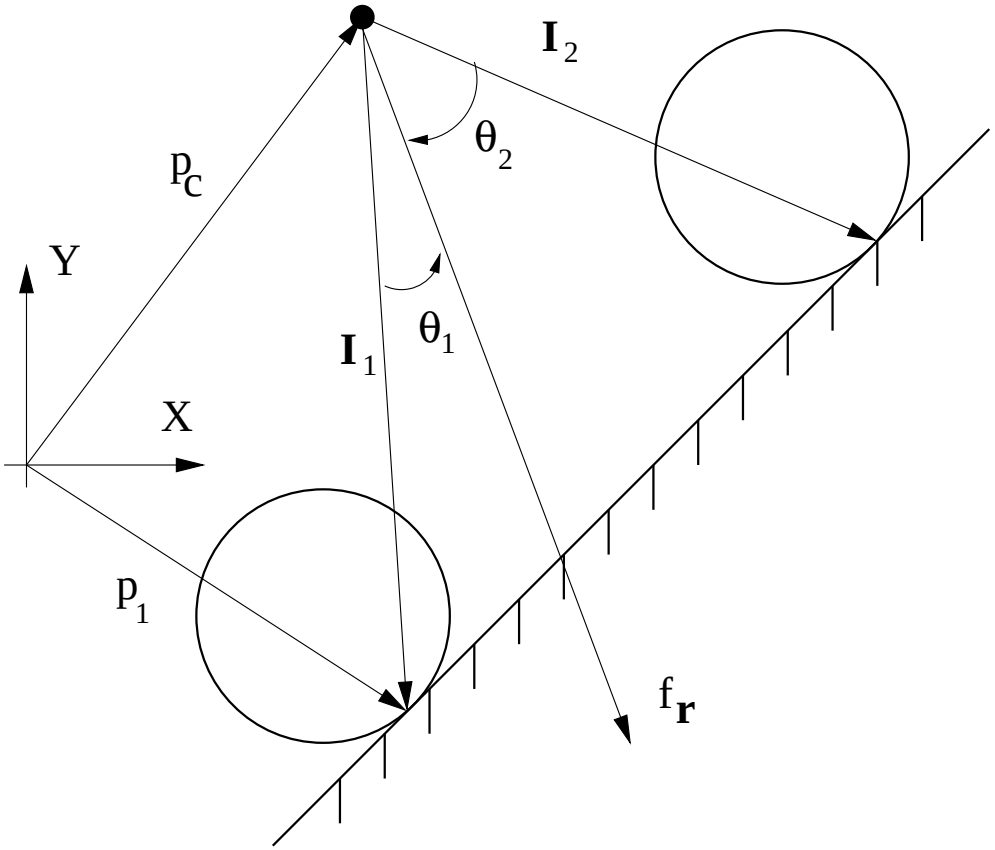


Figure 45: Planar force-angle stability measure

- Centre of mass subjected to a net force $\mathbf{f}_r$.
- $\mathbf{f}_r$ makes angle θ_1 and θ_2 with tip-over axis normals $\mathbf{l}_1$ and $\mathbf{l}_2$.
- Force-angle stability measure
  $\xi = \min\{\theta_1, \theta_2\}||\mathbf{f}_r||$

Force-angle Stability Measure for WMR

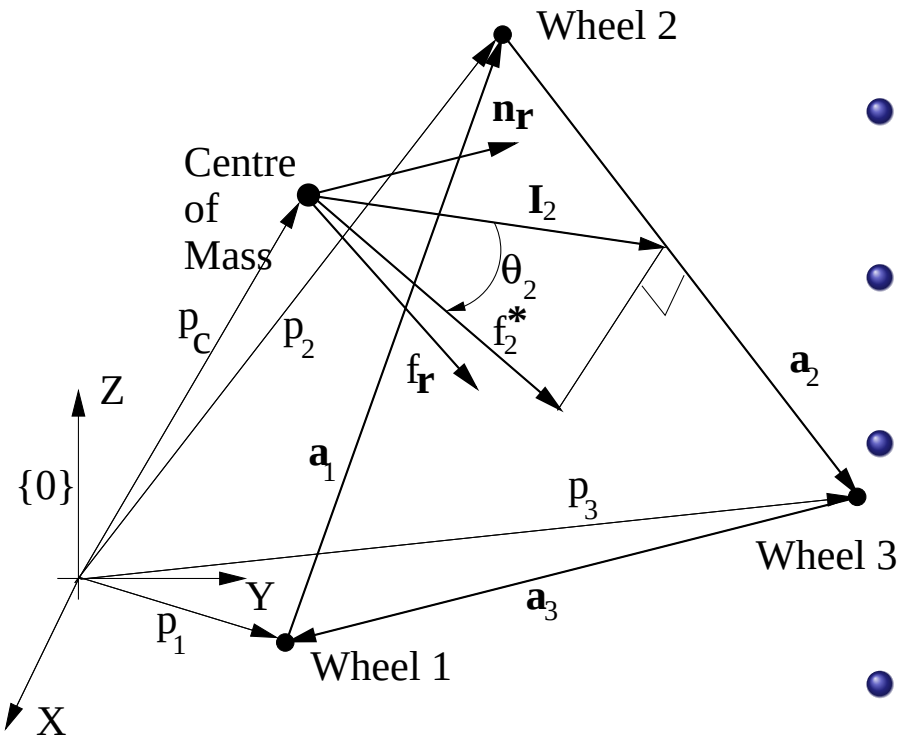


Figure 46: Force-angle stability measure for WMR

- Wheel-ground contact points $\mathbf{p}_i, = (u_{g_i}, v_{g_i}, z_i)^T,\ i = 1,2,3$ known.
- Location of centre of mass $\mathbf{p}_c = (x_c, y_c, z_c)^T$ known in $\{0\}$.
- Line joining wheel-ground contact points $\mathbf{a}_i,\ i = 1,2,3$ are tip-over axis.
- Component of net resultant force is $\mathbf{f}_2^*$ for tip-over axis $\mathbf{a}_2$ (see next slide).
- Angle θ_2 for tip-over axis $\mathbf{a}_2$.
- Likewise find θ_1 for $\mathbf{a}_1$ and θ_3 for $\mathbf{a}_3$.
- If any $\theta_i = 0$, WMR can tip-over $\mathbf{a}_i$.

Force-angle Stability Measure for WMR

- Net resultant force at centre of mass:
  $\mathbf{f}_r = \mathbf{f}_{\text{gravity}} + \mathbf{f}_{\text{dist}} - \mathbf{f}_{\text{inertial}}$
  - Force due to $\mathbf{f}_{\text{gravity}}$ and inertial $\mathbf{f}_{\text{inertial}}$ obtained from dynamic simulation.
  - $\mathbf{f}_{rmdist}$ – External disturbance.
- Net resultant moment at centre of mass:
  $\mathbf{n}_r = \mathbf{n}_{\text{gravity}} + \mathbf{n}_{\text{dist}} - \mathbf{n}_{\text{inertial}}$
- Interested in component $\mathbf{f}_i$ and $\mathbf{n}_i$ about tip-over axis $\mathbf{a}_i$.
- Combine $\mathbf{f}_i$ and $\mathbf{n}_i$ to get a net resultant force
  $\mathbf{f}_i^* = \mathbf{f}_i + \frac{\mathbf{l}_i \times \mathbf{n}_i}{|\mathbf{l}_i|}$, $\mathbf{l}_i$ is the tip-over axis normal.
- Angle for stability measure, θ_i, angle between $\mathbf{f}_i^*$ and unit vector along $\mathbf{l}_i$. Sign of θ_i determines if the net resultant force in *inside* the support polygon or not.
- Overall force-angle stability measure:
  $\xi_i = \min\{\theta_1, \theta_2, \theta_3\} \, ||\mathbf{f}_r||$

Numerical Simulation Results

- Geometry, mass and inertial parameters same as in dynamic analysis
  - Mass of platform = 10 kg and Mass of each wheel = 1 kg.
  - Spring constant = 16.24 Nm/rad and damping = 0.57 Nms/rad.
- Various terrains: Curved path on flat terrain, two rear wheels on two different planes and uneven terrains.
- For each chosen paths and/or input torques, compute at every instant of time t
  - Net resultant force $\mathbf{f}_r$ at centre of mass.
  - Net resultant moment $\mathbf{n}_r$ at centre of mass.
  - Compute tip-over axis $\mathbf{a}_i$ and normal $\mathbf{l}_i$ for $i = 1, 2, 3$
  - Compute $\mathbf{f}_i^*$
  - Compute force-angle stability measure ξ_i.

Numerical Simulation Results – Flat plane

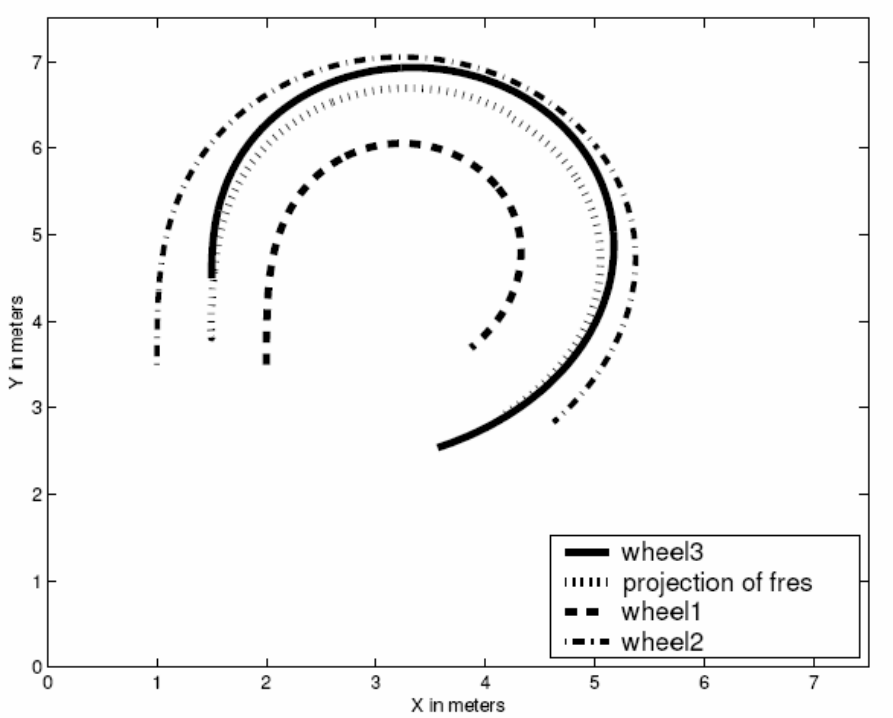


Figure 47: Curve path on a plane

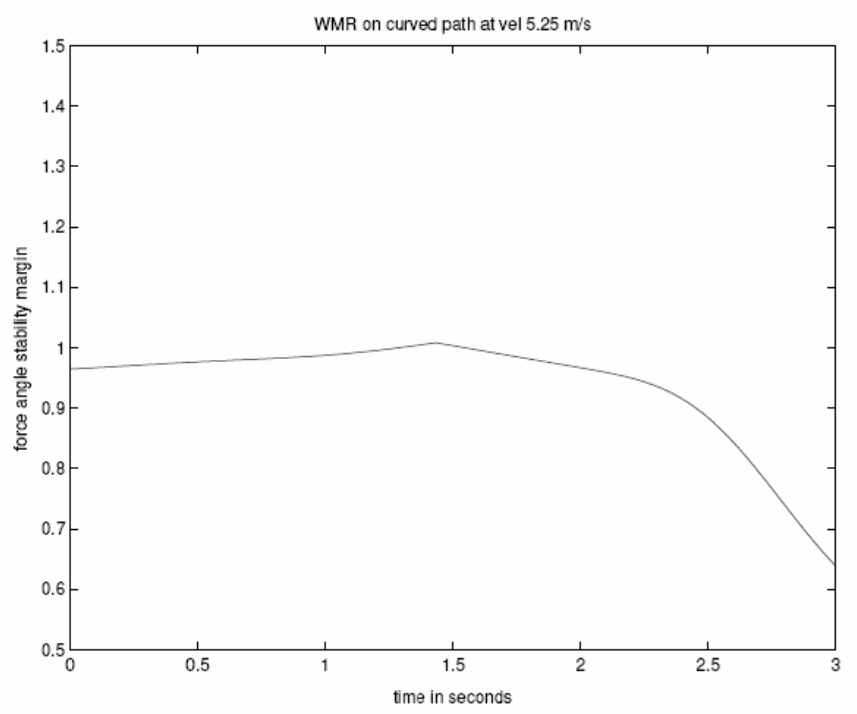


Figure 48: Stability margin for curve path on a plane

- Actuator torques (N-m): $\tau_1 = -0.5$, $\tau_2 = -0.75$, $\tau_3 = -0.004t$.
- As the WMR turns, stability margin reduces.

Numerical Simulation Results – Inclined Plane

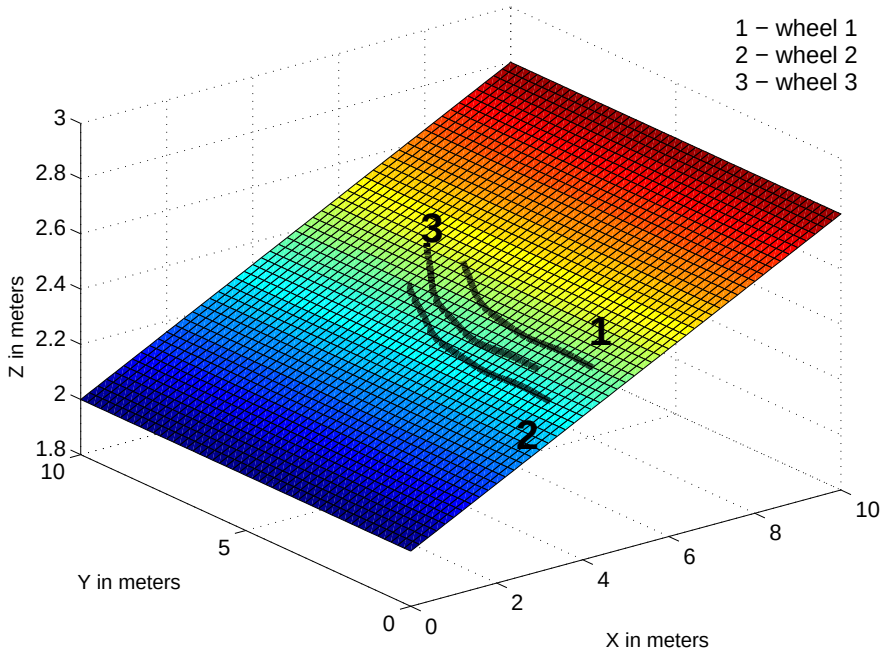


Figure 49: Path traced by WMR on incline plane

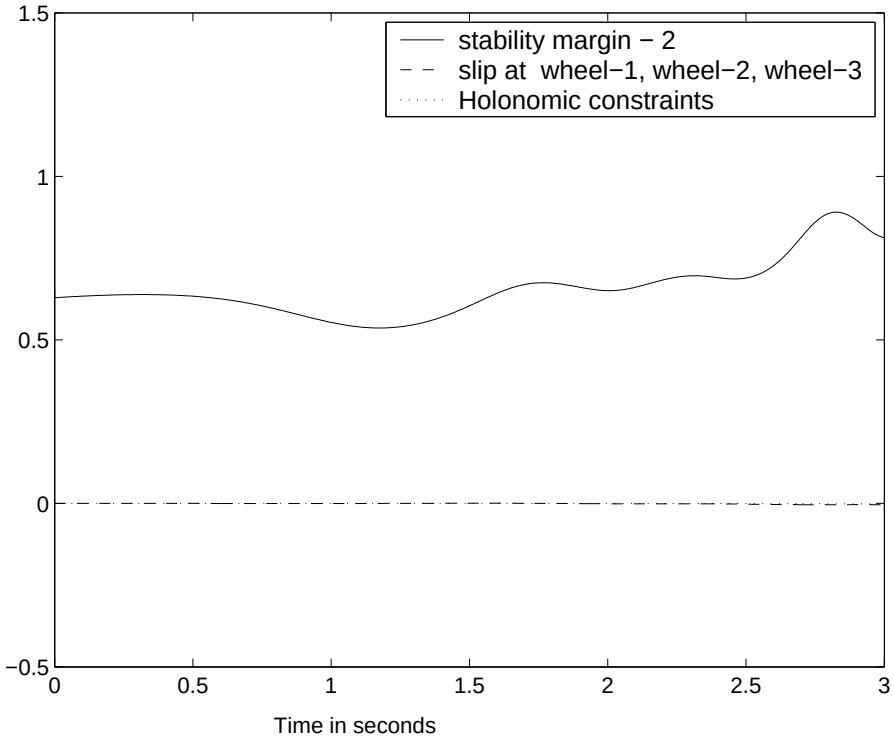


Figure 50: Stability margin for path on an inclined plane

- Input torques (N-m): $\tau_1 = -2.4$, $\tau_2 = -4$, $\tau_3 = -0.08t$.
- Initially least stability about axis 2 – As the WMR turns, tip-over starts shifting from axis 2 to axis 1 $\rightarrow$ Stability increases.

Numerical Simulation Results – Uneven Terrain

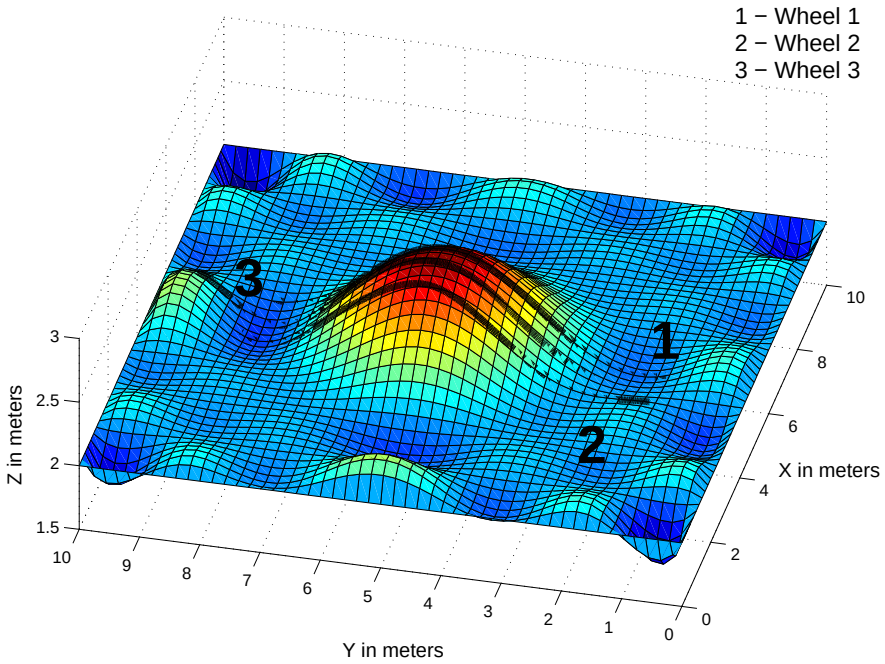


Figure 51: WMR climbing obstacle on a straight path

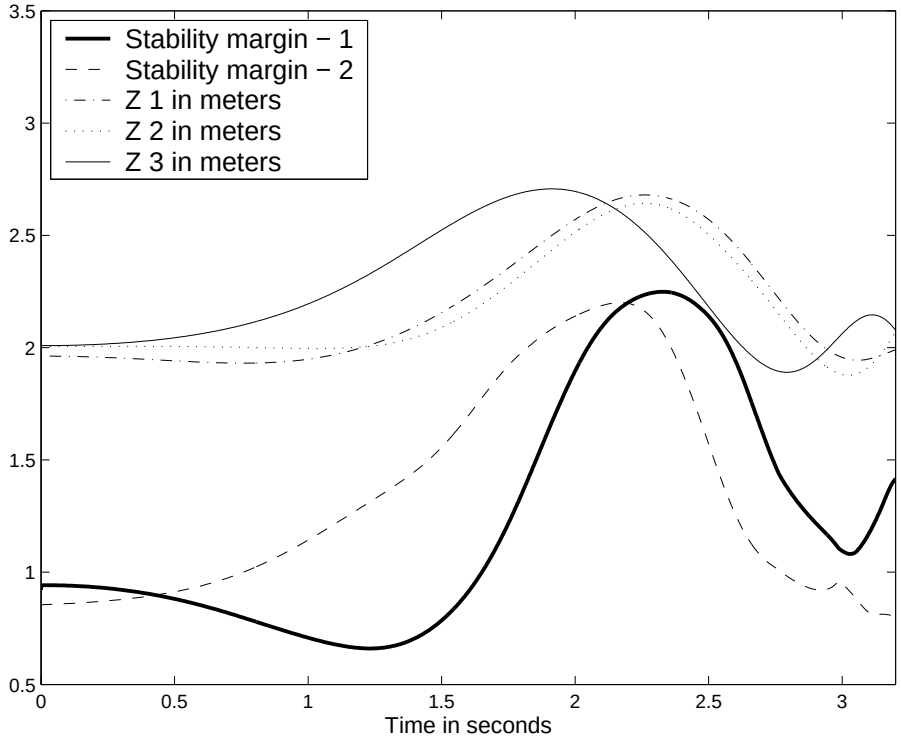


Figure 52: Stability margin along straight path

- Input torques (N-m): $\tau_1 = -4,\ \tau_2 = -4.0,\ \tau_3 = -0.0$.
- WMR is able to negotiate obstacle on uneven terrain without tip-over.

Numerical Simulation Results – Uneven Terrain

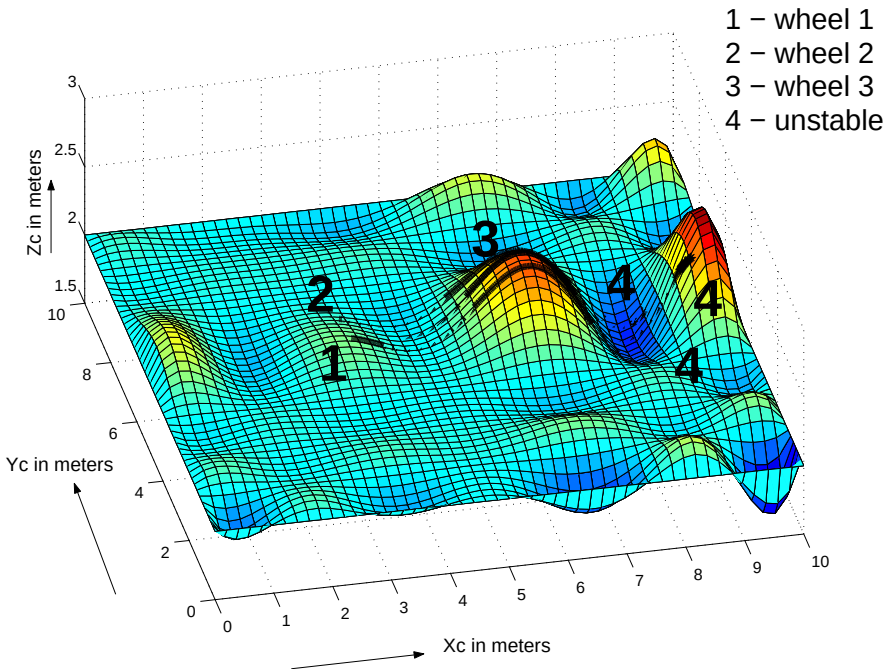


Figure 53: Path traced by WMR on an uneven terrain

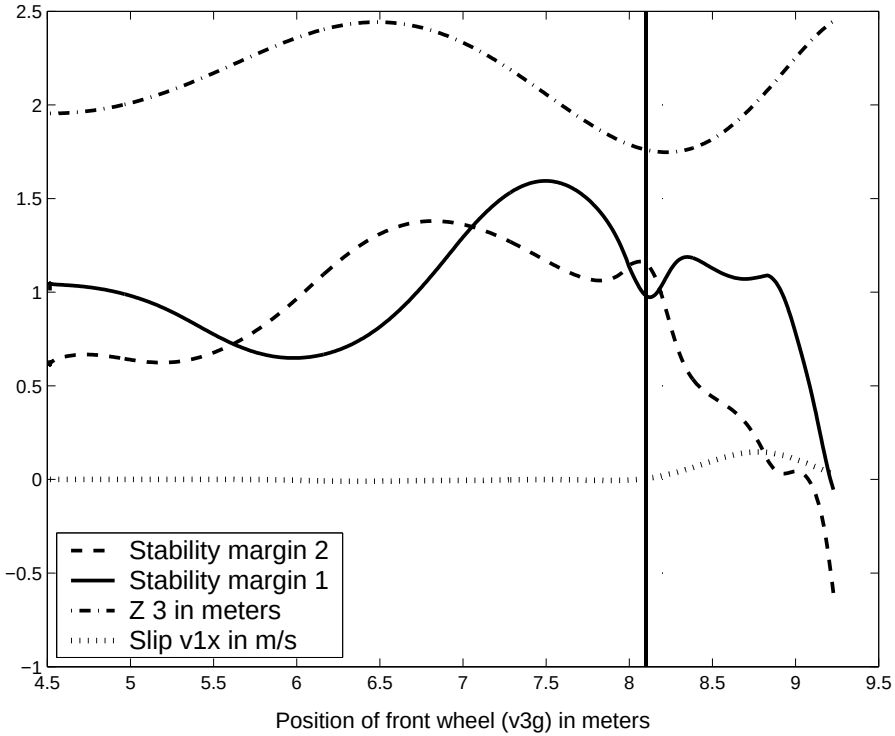


Figure 54: Stability margin on uneven terrain

- Input torques (N-m): $\tau_1 = -4$, $\tau_2 = -4.0$, $\tau_3 = -0.0$.
- ξ reduces while climbing second peak, tip-over occurs about axis 1.
- Simulation *strictly* not valid after the vertical line – Wheel slip increases to more than 10^{-3} m!

SUMMARY

- A three-wheeled mobile robot with torus-shaped wheels.
- Rear wheels with passive lateral tilting capability.
- Modeled as an instantaneous parallel robot with 3 DOF.
- Solution of direct and inverse kinematics by integration.
- Dynamic modeling and simulation.
- Simulation show the capability of traversing uneven terrain without slip.
- Use of force-angle stability measure for tip-over stability.
- Tip-over stability studied for three-wheeled mobile robot for various terrains.

Outline

1. Contents
2. Lecture 1
   - Wheeled Mobile Robots (WMR) on Flat Terrain
3. Lecture 2*
   - Wheeled Mobile Robots (WMR) on Uneven Terrain
4. Lecture 3*
   - Kinematics and Dynamics of WMR on Uneven Terrain
5. Additional Material
   - Problems, References and Suggested Reading

Additional Material

- Simulation movies in ADAMS® for a three-wheeled mobile robot moving on uneven terrain – Movie clip 1 and Movie clip 2[5]
- Exercise Problems
- References & Suggested Reading

- To view above links
  - Copy link and paste in a *New Window/Tab* by *right* click.
  - Close new Window/Tab after viewing.

[5] A three-wheeled WMR moving on uneven terrains was simulated using ADAMS®. The simulation models include a) a WMR platform, b) two torus-shaped rear wheels capable of lateral tilt and a front steered wheel, and c) two-DOF suspension mechanism (at the wheels) required for traversing the uneven terrain. These dynamic simulations are a part of the Ph D thesis of Tharakeshwar A., a student in the Robotics Lab at IISc Bangalore.